

1 **Redefining potentially dangerous glacial lakes in Bhutan by integrating hydrodynamic**
2 **flood mapping and downstream exposure data**

3 Sonam Rinzin^{1,2}, Stuart Dunning¹, Rachel Joanne Carr¹, Simon Allen³, Sonam Wangchuk⁴
4 and Ashim Sattar⁴

5 ¹School of Geography, Politics and Sociology, Newcastle University, Newcastle Upon Tyne,
6 UK

7 ²Department of Geography, University of Zurich, Zurich, Switzerland

8 ³International Centre for Integrated Mountain Development, Kathmandu, Nepal

9 ⁴School of Earth, Ocean and Climate Sciences, Indian Institute of Technology Bhubaneswar,
10 Bhubaneswar, Odisha, India,
11 JBA Consulting, Newcastle Upon Tyne, UK

12

13 **Correspondence: Sonam Rinzin (s.rinzin2@newcastle.ac.uk)**

14 **Abstract**

15 Potentially dangerous glacial lakes (PDGLs) in Bhutan have primarily been identified
16 considering the likelihood of producing a GLOF, which in turn has been assessed only based
17 on upstream lake area/volume and their surrounding topographic conditions. However, this
18 approach is incomplete as it ignores the downstream exposure and vulnerability, and thus the
19 actual impacts. Here, we redefined PDGLs by considering the impact of a simulated GLOF
20 scenario from each lake on downstream exposed elements at risk. Our study shows that a
21 total of approximately 11,322 people, 2,613 buildings, 270 km of road, 402 bridges and 20 km²
22 of farmland are exposed to potential GLOF in Bhutan. We classified lake130 (Thorthormi Tsho)
23 as a very high danger glacial lake in Bhutan, five lakes as high danger and 21 other lakes as
24 moderate danger. Among these high danger glacial lakes, three of them: lake93 (Phudung
25 Tsho), lake251, and lake278 (Wonney Tsho) were not recognized as dangerous in previous
26 studies. Our assessment further revealed that five downstream local government
27 administrative units (LGUs) are associated with very high GLOF danger, while eight others are
28 associated with high GLOF danger. Five of these LGUs had not been previously documented
29 as being at risk from GLOF, including: Chhoekhor and Bumthang town in Bumthang, Paro
30 town and Lamgong in Paro, and Nubi in Trongsa. Our study underscores the significance of
31 integrating potential inundation mapping and downstream exposure data to define dangerous
32 glacial lakes. We recommend strengthening and expanding the existing GLOF preparedness
33 and risk mitigation efforts in Bhutan, particularly in the LGUs, as having high GLOF danger
34 identified in this study, to reduce potential future damage and loss.

35 **1 Introduction**

36 There are currently 110,000 glacial lakes globally, with a total area of ~15,000 km². These
37 glacial lakes have increased in area by ~22% between 1990 and 2020, primarily due to the
38 accumulation of meltwater on newly exposed depressions left by retreating glaciers (Zhang et
39 al., 2024). Glacial lakes across the world have produced 3,152 GLOF events between 850
40 and 2022 C.E. (Lützow et al., 2023), which caused more than 12,400 human deaths and
41 damaged infrastructure worth hundreds of millions of USD (Carrivick and Tweed, 2016; Lützow
42 et al., 2023). In HMA, 682 GLOF events occurred between 1833 and 2022, causing 6,907
43 fatalities (Shrestha et al., 2023). However, this reported number is highly uncertain, primarily
44 because of scarce documentation of the past events. Moreover, ~80% these reported deaths
45 in HMA are associated with a single compounding event involving Chorabari glacial lake and
46 cloud outburst-induced debris flow in 2013 (Allen et al., 2015; Das et al., 2015). Moraine-
47 dammed GLOF events have caused an order of magnitude more damage than the combined
48 damage from all other types of glacial lakes, despite moraine-dammed GLOF events only
49 accounting for one-third of total GLOF events in HMA (Shrestha et al., 2023). This is because
50 GLOFs from moraine-dammed lakes are high magnitude yet episodic, making them highly
51 unpredictable for the downstream settlements (Sattar et al., 2025b; Watanbe and Rothacher,
52 1996). Likewise, moraine-dammed lakes are located in densely populated areas such as the
53 HMA, Andes and Alps, in contrast to other types of glacial lakes, such as ice-dammed or
54 supraglacial ponds/lakes (Emmer, 2024). Thus, it is important to quantify the danger they pose
55 to the downstream settlements.

56 Existing potentially dangerous glacial lakes (PDGLs) in Bhutan are defined based on the
57 likelihood and magnitude of GLOF they will produce, which in turn are assessed based on the
58 inherent stability of the lake's dam and factors that influence the potential for an external
59 triggering event, such as a mass movement entering the lake (Allen et al., 2017; Zheng et al.,
60 2021b). Commonly used parameters include topographic potential for mass input into the lake
61 from the surrounding hillslopes, lake volume (usually derived from a relationship to lake area),
62 lake growth, moraine dam geometry and composition, and catchment area (Zhang et al.,
63 2023b; Zheng et al., 2021b). Although the approaches and factors selected are influenced by
64 study objectives and expert judgment, they are largely based on historical events, often
65 backed with limited observed data (Shrestha et al., 2023). Constraining certain parameters,
66 such as the location and magnitude of possible/probable mass movements entering a lake is
67 challenging even with field-based assessments and more so when using coarse, globally
68 available, open-access data, but the previous studies show that this parameter may be
69 fundamental for the resulting GLOF magnitude (Rinzin et al., 2025). Moreover, the dynamic
70 nature of cryosphere processes, exacerbated under climate warming, means that these

71 reconstructed GLOF characteristics cannot necessarily be applied to contemporary or future
72 conditions (Allen et al., 2017). This is evident from some GLOF events which have occurred
73 from glacial lakes which are deemed less susceptible to GLOF, for example, Lagmale glacial
74 lake in the Nepalese Himalaya in 2017 (Byers et al., 2018) and Gongbatongsha Co lake in
75 2013 in the Indian Himalaya (Cook et al., 2018). Thus, the likelihood of producing a GLOF
76 from any glacial lake is subject to inevitable uncertainties. Most importantly, PDGLs defined
77 solely based on the GLOF likelihood of the lake overlooks how the hydrodynamic properties
78 of a possible GLOF interact with downstream exposure and vulnerability. If a glacial lake
79 generates an exceptionally large flood, but the downstream community is unaffected, we can
80 consider the danger from the glacial lake as low, whereas even a small flood that impacts a
81 large number of people should be classified as high danger. Typically, this is neglected in
82 favour of classifications of danger based only on lake/trigger conditions, and not downstream
83 impacts (Taylor et al., 2023a).

84 In recent decades, the amount of infrastructure, buildings and farmland exposed to potential
85 GLOFs in HMA has increased (Nie et al., 2023). For example, critical infrastructure, such as
86 hydroelectric power plants, is being developed closer to glacial lakes due to growing energy
87 demand in HMA regions (Nie et al., 2021; Schwanghart et al., 2016). In HMA, the population
88 in GLOF-exposed areas increased by 31% (7.0 million to 9.2 million) between 2000 and 2020
89 and may therefore have contributed significantly more towards rising GLOF danger than
90 (debatably) increasing GLOF magnitude due to lake expansion (Taylor et al., 2023b). Thus,
91 changing downstream exposure and vulnerability can play a greater role in shaping
92 contemporary and near-future GLOF risk than the glacial lake and surrounding properties,
93 making the inclusion of the former in the identification of dangerous lakes a crucial, but often
94 overlooked, factor both in the HMA and other high GLOF risk regions globally, such as the
95 Andes (Cook et al., 2016; Colavitto et al., 2024).

96 To identify PDGLs with greater confidence and to implement effective management, mitigation
97 and/or emergency response, we need to consider the interaction between GLOFs,
98 downstream exposure and vulnerability. Taylor et al. (2023a) used the downstream population
99 within a 1 km buffer of the river through which a GLOF would flow, to a maximum runout of 50
100 km from each glacial lake to calculate global-scale GLOF danger. However, the coarse
101 resolution of data and crude assumption of GLOF flow path without hydrodynamic modelling
102 introduces substantial uncertainties due to factors such as detailed local topography,
103 especially where even populations very close in plain view distance to a GLOF flow routeway
104 are in reality disconnected from the river by, for example, high river terraces, which are
105 common in high-mountain regions such as Bhutan. GLOF risk assessments at the HMA scale

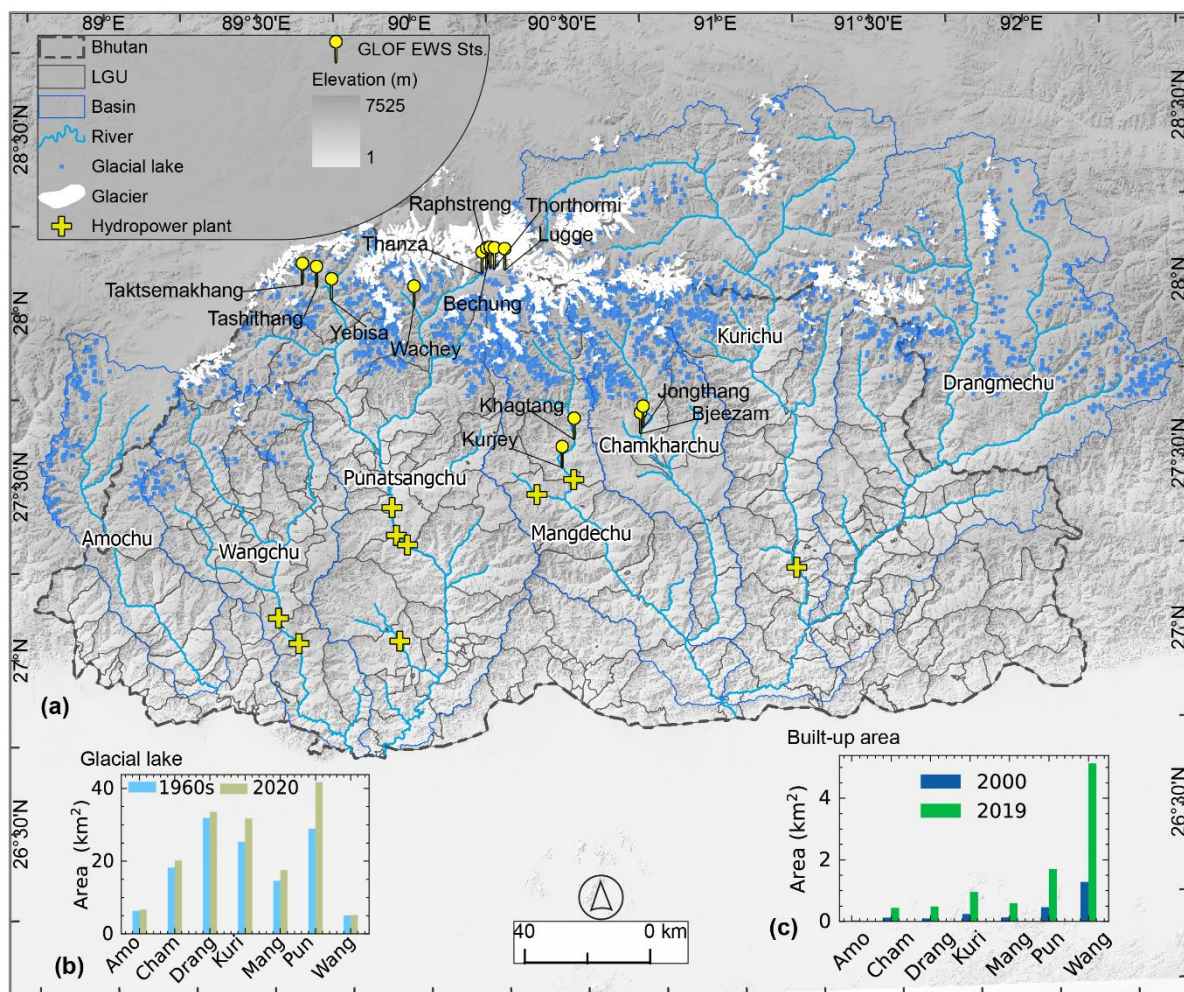
106 have been done by combining hydrodynamic modelling and open-source downstream data,
107 such as OpenStreetMap (Zhang et al., 2023b). Yet, they conducted flood mapping only for the
108 glacial lakes that they deemed very high or high danger through prior GLOF susceptibility
109 assessment. This means that flood mapping for some of the lakes that can directly impact the
110 downstream communities in case of the future GLOF event from these lakes have not been
111 carried out despite huge deviation and inconsistencies between previous susceptibility
112 assessments (Zheng et al., 2021b; Zhang et al., 2023b; Rinzin et al., 2021; National Centre
113 for Hydrology and Meteorology [NCHM], 2019). Moreover, since such studies are focused on
114 a global to continental scale, they do not provide adequate granularity at the national and
115 basin scale for bespoke risk reduction activities and planning.

116 This study presents a new GLOF danger assessment approach for Bhutan, which combines
117 robust flood mapping (through hydrodynamic modelling) and downstream exposure and
118 vulnerability data. For this, we selected all glacial lakes with an area of 0.05 km² (n=278) within
119 the Bhutan Himalaya and conducted hydrodynamic simulations for all these lakes using HEC-
120 RAS (U.S. Army Corps of Engineers, 2021). We then combined the flood map generated
121 through hydrodynamic modelling with downstream data on exposure and vulnerability derived
122 from OpenStreetMap, land-use and land cover maps and population and housing 2017 census
123 data (National Statistics Bureau of Bhutan, 2018). As a result, 1) we produced a flood map
124 for each glacial lake in Bhutan above 0.05 km²; 2) mapped all downstream exposed elements;
125 and 3) provided a new, updated ranking of glacial lakes in Bhutan, based on the danger they
126 pose to downstream settlement(s). We have developed a publicly available web portal that
127 hosts the glacial lake dataset, GLOF inundation maps and downstream GLOF dangers across
128 local administrative units in Bhutan.

129 **2 Study area**

130 Bhutan's landscape is characterised by high mountains, rugged topography and steep terrain
131 with elevations ranging between 200 m a.s.l. in the south to over 7,000 m a.s.l. in the north.
132 Bhutan's northern regions consist of the greater Himalaya mountains, which contain ~1,487
133 km² of glacier ice, of which 64% (951 km²) are debris-covered glaciers (Nagai et al., 2016)
134 (Fig. 1). Between 2000 and 2020, Bhutanese glaciers lost mass at a rate of 0.47 m w.e. yr⁻¹,
135 which exceeds the neighbouring eastern Himalayan (~0.33 m w.e. yr⁻¹) and Nyainqêntanglha
136 (~0.46 m w.e. yr⁻¹) regions (Hugonnet et al., 2021). It is projected that Bhutanese glaciers will
137 undergo continuous and accelerated melting in the future in response to the current climate
138 warming trend (Rupper et al., 2012). As of 2020, there were 2,574 (156.63 ± 7.95 km²) glacial
139 lakes in Bhutan, which was an increase of 17.7% in number and 20.3% in area from the 1960s
140 (Rinzin et al., 2021) (Fig. 1). While these glacial lakes are predominantly present in basins

141 such as Phochu (28.18% of the total lake area) and Kurichu (26.35 % of the total area), they
 142 are widespread across the Bhutan Himalaya and drainage from these lakes flows across most
 143 of the major towns and settlements in Bhutan (Fig. 1). Sixty-four (64) glacial lakes greater than
 144 0.05 km² were identified as highly or very highly susceptible to producing GLOF in the future
 145 based on geomorphological conditions such as topographical potential for avalanching into
 146 the lake (Rinzin et al., 2021). Likewise, using similar criteria, National Centre for Hydrology
 147 and Meteorology (NCHM) has identified 17 PDGLs NCHM (2019) based on the earlier
 148 assessment by ICIMOD (Mool et al., 2001). Of these dangerous glacial lakes, the majority
 149 (n=9) are located within the Phochu basins, the headwaters of Punatsangchu.



150
 151 **Figure 1.** The map (a) depicts Bhutan and the glaciated basins from which the rivers flow into
 152 inland Bhutan. It also shows the distribution of glacial lakes, glaciers, GLOF early warning
 153 monitoring stations (with the names of the places where they are located), and hydropower
 154 plants. The inset bar charts illustrate (b) the glacial lake area in the 1960s and 2020 (Rinzin et
 155 al., 2021) and (c) built-up area changes between 2000 and 2021 as per the land-use and land

156 cover map of ICIMOD (Uddin et al., 2021). The basin names are presented in abbreviated
157 form on x-tick labels for both bar charts.

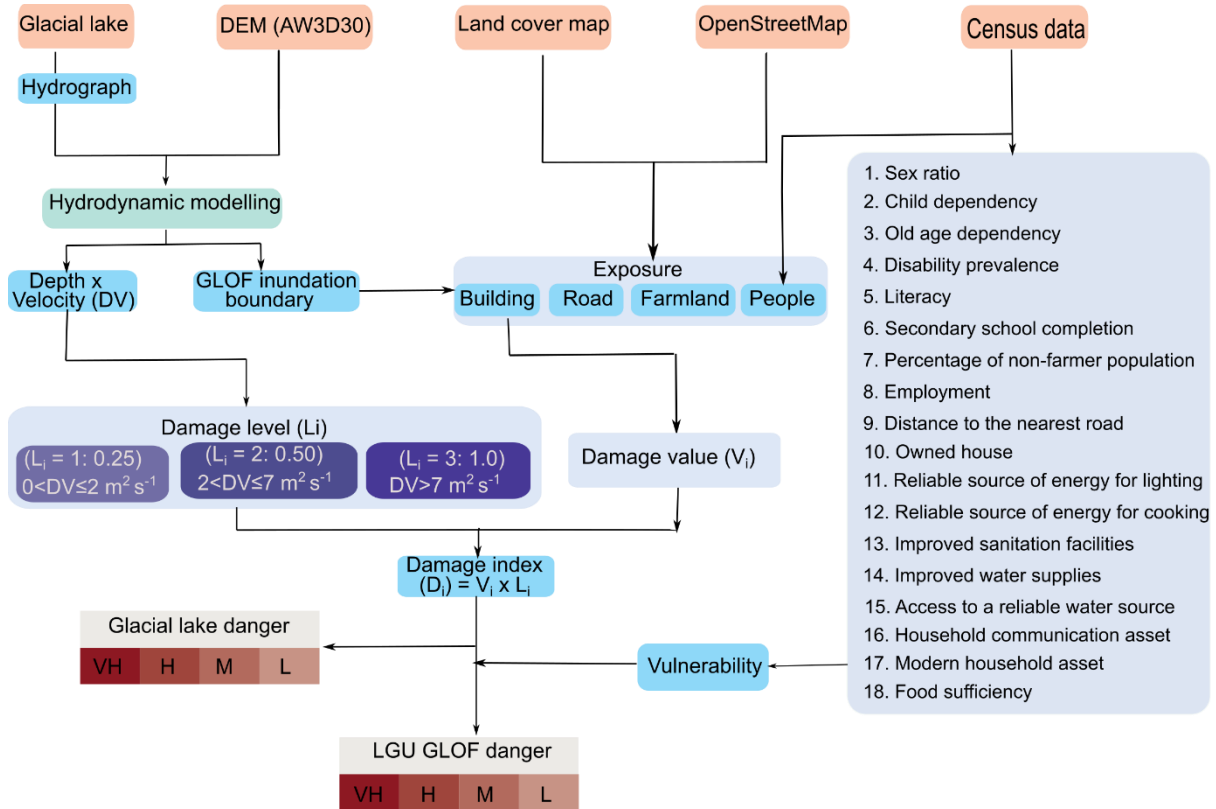
158 The glaciers in the northern mountains feed seven major river systems in Bhutan, namely
159 (West-East): Amochu, Wangchu, Punatsangchu, Mangdechu, Chamkharchu, Kurichu and
160 Drangmechu (Fig. 1). The hydropower generated from these river systems accounts for about
161 40% of Bhutan's national revenue a valued at 0.27 billion USD (Ministry of Economic Affairs,
162 2021), as the majority of energy is being exported to India. All seven currently operational
163 hydropower plants and two nearly commissioned hydropower plants (Punatsangchu-I and
164 Punatsangchu-II) are located along these glacier-fed rivers (Fig.1). The agriculture sector,
165 which is also heavily dependent on these river systems, employs about 60% of the total
166 population (786,385) (National Statistics Bureau of Bhutan, 2018). The built-up areas within
167 the 1 km buffer of these glacier-fed rivers have increased by 200% (2.3 to 9.3 km²) within ~19
168 years from 2000 to 2019 (Fig.1) (Uddin et al., 2021). Thus, infrastructure and crucial economic
169 activity have grown rapidly in areas downstream of glacial lakes in recent decades in Bhutan,
170 making it vital to quantify the danger posed by GLOFs in these basins.

171 **3 Datasets and Methods**

172 **3.1 GLOF modelling hydrodynamic parameters**

173 We used the glacial lake inventory by Rinzin et al. (2021), which has been developed
174 specifically for Bhutan, and which offers greater robustness and accuracy for Bhutan
175 compared to the other datasets available at the Pan-HMA scale (Zhang et al., 2023b; Zheng
176 et al., 2021b). Rinzin et al. (2021) mapped 2,574 glacial lakes in 2020, located within 10 km
177 of glacier termini and with a minimum lake area threshold of 0.003 km². This dataset includes
178 85 transboundary glacial lakes, located in the Indian and Chinese territories of the Himalaya,
179 whose drainage flows into the inland regions of Bhutan. Previous records indicate that GLOF
180 originating from a relatively small lake (as small as 0.001 km²) can cause substantial damage
181 in downstream communities, although such cases are rare. For instance, across HMA region,
182 the median area of glacial lakes with known pre-outburst extents is approximately 0.189 km²
183 (Shrestha et al., 2023). In Bhutan specifically, the smallest glacial lake with a documented
184 outburst history has a present-day area of 0.0506 km² (Rinzin et al., 2021; Komori et al., 2012).
185 Including all glacial lakes for detailed hydraulic modelling would substantially increase the
186 computational demands, whereas resorting to simplified GIS-based approaches (Allen et al.,
187 2019; Zheng et al., 2021b) to cover all lakes would significantly compromise the robustness
188 and accuracy of the resulting flood maps. Therefore, based on the trade-off between model
189 complexity and result reliability, we focused on glacial lakes that (i) are at least 0.05 km² in

190 area and (ii) are located within 1 km of glacier termini. This approach ensures a balance
 191 between computational feasibility and the production of reliable flood maps, while still
 192 capturing a substantial number of potentially dangerous lakes. Based on these criteria, we
 193 identified 278 glacial lakes in Bhutan for flood inundation mapping using hydrodynamic
 194 modelling (Fig. S1).



195
 196 **Figure 2.** Flow chart showing an overview of the methodology we used for assessing GLOF
 197 danger in this study. Here GLOF damage index (D_i) was calculated as a function of damage
 198 value (V_i) and damage level (L_i). The damage index for the local administrative unit (LGU_{di}) is
 199 calculated by further multiplying by the vulnerability index (VL_i). AW3D30 is the abbreviated
 200 form for Advanced Land Observing Satellite (ALOS) Global Digital Surface Model – 30m.

$$V = 42.95 \times A^{1.408} \tag{i}$$

Where V is the volume in 10^6 m^3 and A is the area in km^2

201 Accurate glacial lake volume data is crucial as one of the key determinants of modelled GLOF
 202 hydrodynamic characteristics such as flow depth and velocity. However, field-based
 203 bathymetric measurement for multiple lakes is costly and not currently possible for some
 204 glacial lakes due to their remote location. In the absence of in-situ bathymetric data to
 205 determine volume, we calculated the volume of each glacial lake using the area-volume
 206 scaling relationship (equation (i)) proposed by Zhang et al. (2023a) based on the area of each

207 glacial lake as mapped in 2020 (Rinzin et al., 2021) (See table S1). This area-volume scaling
208 relationship, based on recent bathymetric data from the Greater Himalayan region, including
209 13 representative lakes from Bhutan, is well-suited to approximate Bhutanese glacial lake
210 volumes (Zhang et al., 2023a).

211 It is important to note that not all lakes drain entirely during a GLOF (Maurer et al., 2020; Nie
212 et al., 2018; Zhang et al., 2024). The amount of water drained during a GLOF event depends
213 on numerous factors, such as dam geometry and composition, lakebed topography, and
214 potential triggers. While consideration of all these factors is crucial for a detailed impact
215 assessment of a particular glacial lake, constraining the volume based on these detailed
216 attributes is highly challenging for a study involving numerous glacial lakes. Previous data
217 indicate that smaller lakes are more likely to drain completely during a GLOF event than larger
218 lakes. Here, we used data from Zhang et al. (2023b) documenting the drainage volumes of 64
219 lakes in the HMA regions. Among these 64 lakes, the median percentage of drainage volume
220 was 98% for lakes with an area < 0.1 km², 62% for lakes with an area of 0.1 to 1 km² and 33%
221 for lakes with an area >1 km². We used these observed drainage percentages as the basis to
222 calculate the flood volume generated by each lake. For simplicity and recognizing that these
223 median drainage values lie within the uncertainty bounds of established area-volume scaling
224 relationships, we adopted the following assumptions: 100% drainage for lakes < 0.1 km², 60%
225 drainage for lakes between 0.1 and 1 km², and 30% drainage for lakes > 1 km². Subsequently,
226 we used Evans's empirical equation (ii) for moraine-dammed lakes to calculate the possible
227 peak discharge of each lake (Evans, 1986). See supplementary Figure S1 for the distribution
228 of volume and peak flow calculated for each glacial lake in Bhutan (see Table S1).

$$Q_{max} = 0.72V^{0.53} \quad (ii)$$

Q_{max} is peak discharge, and V is the total volume of the lake calculated using equation (i)

229 **3.2 HEC-RAS model set-up**

230 Most GLOFs from moraine-dammed lakes start from dam breaching, which is frequently
231 triggered by large mass movement(s) entering the lake from the surrounding terrain hillslopes
232 (Shrestha et al., 2023). However, conducting a dam breach simulation for each lake is
233 challenging due to complexities and uncertainties in constraining the appropriate value for
234 a large range of input parameters (U.S. Army Corps of Engineers, 2021). To simplify this, we
235 conducted a flood simulation resulting from each lake by using an input hydrograph as
236 an upstream boundary condition. For each lake, we generated an input hydrograph by fitting
237 the peak flow of each lake to the log-normal distribution curve with a standard deviation
238 (sigma) value of 0.75 and a mean of 0, adapting the approach used by the earlier studies (Carr

239 et al., 2024; Kropáček et al., 2015). For example, for lake1, the peak flow was $1,110 \text{ m}^3 \text{ s}^{-1}$,
240 thus, we constructed a log-normally distributed hydrograph with a peak flow of $1,110 \text{ m}^3 \text{ s}^{-1}$
241 and gradually decreased the flow after reaching this peak flow. With this assumption, we
242 generated the hydrograph so that the flow rises to its peak rapidly and progressively decreases
243 after attaining the peak, which is consistent with the hydrograph of many previous GLOF
244 events (Maurer et al., 2020; Nie et al., 2020; Zheng et al., 2021a) (see supplementary Figure
245 S2 for a representative hydrograph). The flow duration of the hydrograph of each lake was
246 subsequently adjusted to account for the complete drainage of the estimated drainage volume
247 calculated for each lake. For example, for lake1, the required drainage volume was calculated
248 at $1.036 \times 10^6 \text{ m}^3$, and so, the flow duration for this lake was adjusted so that the cumulative
249 flow through the GLOF event was equal to this volume (Table S1).

250 We used the ALOS Global Digital Surface Model (AW3D30) with $\sim 30 \text{ m}$ ground resolution as
251 a source of terrain information for the model setup (Japan Aerospace Exploration Agency,
252 2021). We chose AW3D30 because various previous studies (Rinzin et al., 2025) have
253 indicated that it has higher vertical and horizontal accuracy compared to other freely available
254 DEMs over our study area with similar spatial resolution, such as SRTM GL1 (for example,
255 Liu et al. (2019). Chow (1959) suggested Manning's Coefficient (n) between 0.040 to 0.070
256 for the river channel bed with large boulders and cobbles, which closely characterise the river
257 channels in the Bhutan Himalaya. Thus assigned n value of 0.06 which has been used in
258 GLOF modelling in Bhutan previously (Maurer et al., 2020).

259 We created one HEC-RAS project for each major river basin so that a total of seven project
260 files correspond to the seven glaciated basins in Bhutan. For each project, the model domain
261 was established by creating a 1,000 m buffer on either side of the centre line of the river
262 originating from each lake. Within this model domain, a computational mesh with a grid
263 resolution equal to the native resolution of AW3D30 ($30 \times 30 \text{ m}$) was generated. An upstream
264 boundary condition for each lake was defined at the frontal terminus of each lake. However,
265 we used the same downstream boundary condition for all lakes in the basin, which were
266 defined at the furthest end at the international border between Bhutan and India (for example,
267 Fig. S2). Likewise, unique flow data was created for each lake, where we imposed flow
268 hydrographs as the upstream boundary condition for the respective lake and downstream
269 boundary conditions defined by normal depth with an energy slope of 0.01 (U.S. Army Corps
270 of Engineers, 2021). Finally, one unsteady flow analysis plan for each lake with corresponding
271 unsteady flow data and boundary conditions was developed. For example, in the Phochu
272 basin, which contains 67 glacial lakes considered for this study, one project file was
273 established. This project file included a single model domain, a downstream boundary

274 condition, 67 upstream boundary conditions and 67 flow datasets. Accordingly, we created 67
275 individual plans, each featuring the respective upstream boundary, uniform downstream
276 boundary condition and flow data that contains the specific hydrograph for each lake (Fig. S2).

277 We computed all the simulations using the full momentum shallow water equations since they
278 better represent GLOF rheology than the diffusion wave equation (Sattar et al., 2023; Sattar
279 et al., 2021). Considering that this study is mainly aimed at providing a GLOF danger overview
280 at the Bhutan scale, all other computational parameters were maintained at the default setting.
281 At a mesh size of 30 m, each model was run stably with a computational time step of 3 seconds
282 within a Courant number well below 2 (U.S. Army Corps of Engineers, 2021). The simulations
283 were executed simultaneously across 15 computers at the Geospatial Laboratory in
284 Newcastle University. We maintained 10 hours of simulation time for each model setup, which
285 took 2 to 4 hours depending on the lake's size. Output for each project plan was carefully
286 examined and any models exhibiting instability (e.g., a Courant number above 2 or failed
287 before complete execution) were re-executed by adjusting the position of upstream boundary
288 condition, changing the timesteps and adding additional features like refinement regions within
289 the 2D model domains to ensure stable model run and reliable results (U.S. Army Corps of
290 Engineers, 2021).

291 **3.3 GLOF impact and exposure**

292 We collated the GLOF inundation boundary for each lake generated through HEC-RAS
293 modelling and calculated the area and length of each inundation. We mapped all buildings,
294 roads, bridges, farmland, and hydropower plants within the GLOF inundation area to identify
295 downstream elements at risk. The OpenStreetMap (updated as of 30-04-2025) was used to
296 map buildings, roads and bridges. We manually verified the OpenStreetMap data using
297 Google Earth high-resolution imagery and updated 41 km of missing roads, 152 buildings and
298 20 bridges using Google Earth imagery within the flood inundation plain. The local government
299 administrative unit (LGU) boundary map was then used to map these elements at risk in each
300 LGU. However, there is no population data with sufficient granularity to map exposed people
301 directly. We therefore used exposed buildings as a proxy for exposed people, assuming that
302 the distribution of people usually corresponds to the location of buildings. Specifically, we
303 divided the total population of each LGU by its total number of buildings, using the 2017
304 Bhutan population and census data (National Statistics Bureau of Bhutan, 2018) and
305 OpenStreetMap building data. The number of people exposed to GLOF in each LGU was then
306 calculated by multiplying the population per building by the total exposed buildings. The
307 ICIMOD's Landsat-based land-use and land cover map of 2023 was used to map farmland
308 (Uddin, 2021) since it is of better quality at the HKH scale than other open-access land cover

309 data, such as Esri Sentinel-2 land cover data (Karra et al., 2021). We considered buildings the
310 most important downstream exposed element because they are the primary space where
311 people live. Thus, we used exposed buildings to calculate the GLOF damage index (Fig. 2).

312 **3.4 GLOF damage and danger**

313 In this study, we defined a GLOF danger based on the downstream damage (calculated here
314 as damage index (D_i)) resulting from each GLOF event (Fig. 2). The term 'danger' is adopted
315 in this study instead of 'hazard' and 'risk' as our assessment does not account a probability
316 component of hazard following the convention used in the earlier studies (Taylor et al., 2023a;
317 Allen et al., 2019). The danger in this study refers to damage/destruction to buildings that could
318 results from future potential GLOF. We assume that any of our study glacial lakes has the
319 potential to generate a GLOF in the future, and the resulting damage will determine how
320 danger that the glacial lake would be to those downstream communities. The D_i for each
321 element (grid cell) resulting from any GLOF event was calculated as a function of the value of
322 the exposed element (V_i) and the level of damage (L_i) following the approach proposed by
323 Petrucci (2012) (equation (ii)) (Fig. 2). Qualitative data such as construction type, occupancy,
324 and value of the content of the building inside the house are essential to obtain the appropriate
325 value of structure and content. However, such qualitative attributes are incomplete in the
326 existing OpenStreetMap and introduce substantial uncertainties when estimated using other
327 open-access data. In this study, our focus is on providing a relative quantitative comparison of
328 GLOF impacts across different communities instead of determining exact damage values
329 resulting from each GLOF event. Therefore, we considered each building as one unit of V_i
330 uniformly applied across the study domain (Fig. 2).

331 GLOFs with higher water flow velocity can cause more damage to the downstream elements
332 than slow-flowing water (Federal Emergency Management Agency, 2004). Therefore, we
333 calculated the L_i associated with each GLOF event as a function of both velocity and depth,
334 which was accomplished by calculating the depth \times velocity (DV) from the HEC-RAS output
335 layer. The level of damage a building suffers also depends on its structural integrity, which in
336 turn is a function of the construction type of the building. The 2017 Bhutan Population and
337 Housing Census reported that the construction type of most Bhutanese buildings is masonry
338 (National Statistics Bureau of Bhutan, 2018). Clausen and Clark (1990) have categorized three
339 damage levels to masonry buildings based on DV as follows: inundation ($DV \leq 2 \text{ m}^2 \text{ s}^{-1}$), partial
340 damage ($2 \text{ m}^2 \text{ s}^{-1} < DV \leq 7 \text{ m}^2 \text{ s}^{-1}$) and complete damage ($DV > 7 \text{ m}^2 \text{ s}^{-1}$). Accordingly, we
341 used these DV value ranges to classify three levels of damage and assigned L_i following
342 Petrucci (2012) as follows: Level 1 ($L_i = 0.25$), Level 2 ($L_i = 0.5$), and Level 3 ($L_i = 1$) (Fig. 2).

343 Finally, D_i for all damaged grid cells located within the GLOF inundation boundary of each lake
 344 were summed to derive an danger value (D_g) associated with each lake (equation (iii)). The
 345 D_g was then normalized between 0 and 1, and lakes were ranked based on this metric.
 346 Additionally, for the classification purpose, using normalized D_g , we categorized glacial lakes
 347 into four danger levels: very high danger, high danger, moderate danger, and low danger using
 348 the Natural Jenks classification system in ArcGIS.

$$D_g = \sum_{i \in g} D_i = \sum_{i \in g} V_i L_i \quad (\text{iii})$$

Where D_i is the damage index for exposed element i , V_i is the value of each downstream element, and L_i is the damage level for each element. D_g is the aggregated damage index for geographical unit g (LGU or inundation boundary of the respective lake)

349 **Table 1.** Socio-economic indicators used to calculate LGUs' vulnerability to the future GLOF.
 350 The indicators were extracted from Bhutan's 2017 population and housing census. Details on
 351 how data for each indicator are collected are provided in the National Statistics Bureau of
 352 Bhutan (2018). The calculated values were inverted so that they contribute positively to
 353 vulnerability for the indicators other than child dependency, old age dependency, and disability
 354 prevalence rate.

Indicator	Definition
Sex ratio	Number of males to every 100 females
Child dependency	The ratio of the number of children aged 0 to 14 years to population aged 15 to 64
Old age dependency	The ratio of persons 65 years and above to the population aged 15 to 64 years
Disability prevalence	The proportion of the population with a disability
Literacy	The ratio of the literate population (read and write in Dzongkha and English) aged 6 years and above to the total population of the same age group
Secondary school completion	The ratio of persons aged 6 years and above who have completed secondary education (grade XII) to the population of the same age group, expressed as a percentage
Percentage of non-farmer population	Percentage of people aged 15 years and above who are employed in sectors other than farming
Employment	Percentage of persons aged 15 years and above who are employed
Distance to the nearest road	Proportion of households within a 30-minute walk of the nearest road point
Owned house	Proportion of households living in an owned house
Reliable source of energy for lighting	Proportion of households with a main source of energy for lighting as electricity

Reliable source of energy for cooking	Proportion of households with a main source of energy for cooking as electricity
Improved sanitation facilities	Proportion of households with improved sanitation facilities
Improved water supply	Proportion of households with water supplies inside the dwelling
Access to a reliable water source	Proportion of households with a water available at least during the critical times (5:00–8:00, 11:00–14:00 and 17:00–21:00), adequate for washing and cooking
Household communication asset	Proportion of households owning communication and media facilities
Modern household asset	Proportion of households with modern household assets
Food sufficiency	Proportion of households having sufficient food to feed all the household members during the last 12 months

355 **3.5 Downstream exposure and danger**

356 We conducted GLOF damage assessment for downstream settlements at various
357 geographical scales: 20 districts and 274 local government administrative units (LGUs)
358 (including 205 gewogs [sub-district blocks] and 69 towns). We aggregated the D_i of each
359 damage grid located within the respective LGU boundary to calculate D_g for each LGU using
360 equation (iii). In cases where downstream elements were affected by GLOFs originating from
361 multiple lakes, the combined D_g from each contributing lake was considered in the analysis to
362 account for their exposure to multiple possible GLOFs (Fig. 2).

363 As well as the magnitude of GLOF and the presence of downstream elements along the flow
364 path, downstream GLOF danger is also determined by the community's capacity to prepare,
365 respond and recover from a GLOF event (Cutter et al., 2008; Zhou et al., 2009). Lack of this
366 capacity, referred to as vulnerability, is influenced by wide-ranging socio-economic factors,
367 including but not limited to the standard of living and gender composition of the community
368 (Cutter and Finch, 2008). Across the world, developed countries were found to be more
369 disaster resilient than developing countries, while disaster-related death and damage have
370 largely spiked in low-income countries (Rahmani et al., 2022). However, identifying specific
371 socio-economic variables that are most relevant to GLOF damage remains a significant
372 challenge, particularly because social data from past events are either unknown or, at times,
373 overlooked. Past studies have used variables such as gross domestic product, population
374 density (Carrivick and Tweed, 2016), human development index, corruption index and social
375 vulnerability index at the national scale (Taylor et al., 2023a). While such data represent a
376 broad overview of the country's socio-economic condition and thus vulnerability to disaster,
377 they do not represent the regional and community-level disparity within the country that
378 influences their ability to respond and recover from the disaster. To address this, drawing upon
379 our local understanding and following earlier studies (Allen et al., 2016; Rinzin et al., 2023),
380 we calculated the relative vulnerability index using a total of 18 socio-economic indicators from

381 the 2017 Bhutan population and housing census (National Statistics Bureau of Bhutan, 2018)
382 (Table 1). This census data, which is updated every 10 years, represents the most
383 comprehensive and detailed dataset currently available, offering spatial granularity at the
384 individual LGU level. These indicators are essential for evaluating a community's
385 preparedness and response capacity to disasters from hazards like GLOF (Cutter and Finch,
386 2008). For example, in Bhutan's traditionally gendered societal structure, men often assume
387 more prominent roles in disaster response efforts. The vulnerability index for each LGU was
388 calculated as the normalised value across these 18 socio-economic indicators (Fig. 2). The
389 definitions and approaches used for calculating each indicator are summarized in Table 1.
390 Assuming that the LGUs with higher vulnerability index are less able to respond to and recover
391 from a future GLOF, D_g for each LGU was multiplied by vulnerability index.

392 **3.6 GLOF arrival time and GLOF early warning system**

393 Building damage from GLOF is a function of hydrodynamic factors such as depth and velocity,
394 and the structural integrity of the buildings. On the other hand, human casualties and injuries
395 also depend on the warning/response time, making it essential to consider flood arrival time
396 in GLOF danger assessment. Thus, GLOF arrival time needs to be considered separately
397 from the D_i we computed earlier. Accordingly, we determined the flow arrival time of the earliest
398 arriving GLOF for each LGU to determine the amount of response time the people living in the
399 particular LGU will get in case of future GLOF.

400 The NCHM (NCHM), Bhutan, monitors several lakes in Bhutan identified as dangerous
401 (NCHM, 2019). Currently, they have a GLOF early warning system covering Punatsangchu,
402 Mangdechu and Chamkharchu basins, which consists of 23 monitoring stations (Fig. 1). We
403 utilized monitoring station location data from NCHM to evaluate the relationship between
404 Bhutan's existing early warning system, modelled GLOF scenarios originating from these
405 glacial lakes and affected downstream communities. To achieve this, we first overlaid all
406 monitoring stations in Bhutan using ArcGIS and counted how many of our catalogue of
407 possible GLOFs in the region are covered by the existing early warning system based on their
408 hydrological relationship (NCHM, 2021). We assumed that if a GLOF flow intersects any of
409 the existing EWS monitoring stations, then the event would be monitored by the existing EWS
410 in Bhutan. Similarly, if an LGU is affected by a GLOF that passes through one or more of these
411 stations, the LGU is regarded as being monitored by the existing EWS.

412 **3.7 Sensitivity analysis**

413 Hydraulic modelling is complex, relying on numerous input parameters, some of which are
414 difficult to constrain even with novel field observation data. However, conducting sensitivity
415 analysis for every parameter is highly challenging and deemed unnecessary within the scope

416 of this study, given the scale of GLOF modelling conducted in this study. Here, we therefore
 417 focused on Manning's coefficient value and the area of glacial lakes for the sensitivity analysis.
 418 n is a well-established sensitive parameter in hydraulic modelling with HEC-RAS 2D, and the
 419 area of the lake is essential in our study, as we used it as a proxy for calculating volume and
 420 peak discharge using an empirical equation. We examined the interaction impact of n and
 421 area of glacial lake variation by modelling 20 scenarios of GLOF, combining four different n
 422 (0.04, 0.05, 0.06, 0.07 as suggested by Chow (1959) for cobble beds with large boulder for
 423 mountain stream) and five different scenarios of glacial lake area (0.01, 0.05, 0.1, 1, 5 km²).
 424 We assessed how these interactions affect DV , the main hydraulic metric we used for
 425 assessing downstream damage from the future potential GLOF.

426 **Table 2.** GLOF exposed elements: people, buildings, roads, bridges and farmland distributed
 427 across the top 20 GLOF LGUs. The total value in the last row represents the total exposed
 428 elements across all LGUs in Bhutan.

Gewog/Town	District	Building (count)	Population (count)	Road (km)	Bridge (count)	Farmland (km ²)	Rank
Chhoekhor	Bumthang	192	321	41.6	36	0.28	1
Punakha Town	Punakha	272	1635	10.8	4	1.14	2
Lunana	Gasa	121	232	39.9	30	0.00	3
Thedtsho	Wangdue Phodrang	165	705	3.59	6	0.90	4
Bumthang Town	Bumthang	283	864	13.2	2	2.32	5
Khatoed	Gasa	17	16	0.42	4	0.00	6
Toedwang	Punakha	60	98	4.97	8	1.08	7
Nubi	Trongsa	29	53	1.95	8	0.30	8
Lamgong	Paro	195	541	7.86	6	0.85	9
Paro Town	Paro	262	1748	13.2	12	1.14	10
Darkar	Wangdue Phodrang	85	1936	3.22	16	0.31	11
Lingmukha	Punakha	65	90	5.74	2	0.19	12
Dzomi	Punakha	53	134	6.22	6	1.22	13
Wangdue Phodrang Town	Wangdue Phodrang	109	1059	1.19	0	0.25	14
Sharpa	Paro	120	370	3.75	8	0.94	15
Toedtsho	Yangtse	13	20	0.39	0	0.09	16
Athang	Wangdue Phodrang	38	54	2.04	10	0.42	17
Khoma	Lhuentse	42	87	6.68	8	0.04	18
Gase	Wangdue Phodrang	37	156	3.76	8	0.26	19
Tshogongm Langthil	Trongsa	11	38	1.26	8	0.82	20
Total		2,613	11,322	264	362	19	

429 **4 Results**

430 **4.1 Flood volume and peak discharge**

431 Of the 278 glacial lakes selected for GLOF modelling and downstream danger assessment in
432 this study, the majority (n= 91) of them were in the Punatsangchu basin, followed by the
433 Kurichu basin (n=64). By contrast, Wangchu (n = 2) and Amochu (n=5) had the minimum
434 number of lakes meeting our selection criteria (Fig. 3). The total volume the selected glacial
435 lakes ranged between $0.64 \times 10^6 \text{ m}^3$ to $344.1 \times 10^6 \text{ m}^3$ with a median volume of $2 \times 10^6 \text{ m}^3$.
436 Based on these total volumes, minimum, median and maximum drainage volumes were 0.64
437 $\times 10^6 \text{ m}^3$, $1.4 \times 10^6 \text{ m}^3$ and $103.2 \times 10^6 \text{ m}^3$, respectively. Furthermore, the empirical-based
438 estimation showed that these glacial lakes can produce GLOFs with peak discharges of up to
439 $24,085 \text{ m}^3 \text{ m}^{-1}$, while the median peak discharge is $1,552 \text{ m}^3 \text{ m}^{-1}$ (Fig. S3).

440 **4.2 GLOF impact and exposure**

441 Our study revealed that GLOFs from individual glacial lakes can travel as far as 167 km
442 downstream and can inundate a maximum area of 30 km^2 . The modelled GLOFs exhibit a
443 median travel distance of 40 km and an inundation area of 2.9 km^2 (Fig. S3). Collectively,
444 about 2% (781 km^2) of Bhutan's total land area is exposed to GLOF. The mean flow depth and
445 velocity were 3.3 m and 3.4 m s^{-1} , respectively (Fig. S4). The shortest arrival time to the
446 nearest building was 8 minutes, and the longest was 10 hours (Fig. S3). As a result, a total of
447 11,322 people, 2,613 buildings, 270 km of road, 402 bridges, 19 km^2 of farmland and 4
448 hydropower dams are exposed to GLOFs in Bhutan (Table 2). Of the total modelled GLOF
449 events, 71% (n = 197) affect roads, 42% (n = 116) affect buildings, and 28% (n = 77) affect
450 farmland. The rest of the GLOFs do not affect any downstream entities. A GLOF from Bhutan's
451 most dangerous lake, Thorthormi Tsho, could impact 1,119 buildings, 72 km of roads, and 4.2
452 km^2 of farmland, making it the most consequential event for reaching elements at risk. It is
453 followed by lake278, located in the Wangchu basin and Chubdha Tsho in the Chamkharchu
454 basin, both of which are classified as high danger glacial lakes by this study (Table S1).

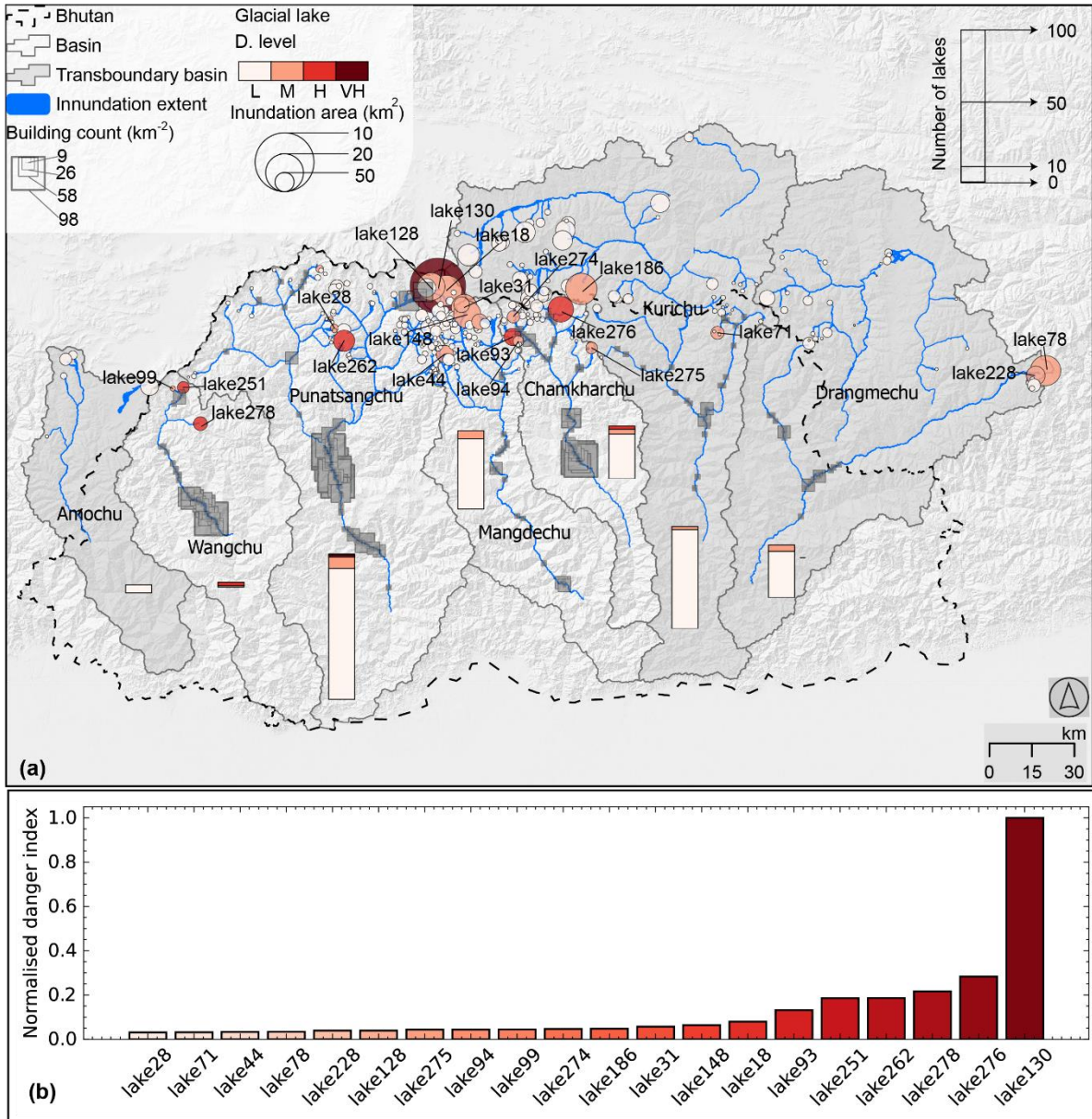
455 Out of 278 glacial lakes selected for flood mapping for this study, 85 (30.6%) are within
456 catchments that cross the boundaries of India and China and drain into Bhutan inland. GLOFs
457 from these transboundary lakes also affect a substantial number of downstream elements
458 located in Bhutan, including 20 buildings, 0.6 km^2 of farmland, and 2 km of roads in Bhutan.
459 All these exposed elements are situated within the Kurichu and Drangmechu basins.

460 The exposed elements are distributed across 17 districts and 88 local government
461 administrative units (LGUs). Bumthang, Paro, Punakha, Wangdue Phodrang and Gasa
462 districts are most affected by the GLOFs. For example, Paro itself has 673 GLOF exposed
463 buildings, 32 km of road and 64 bridges (Table 2). Among the LGUs, the maximum exposed

464 building is in Bumthang town (n= 283), followed by Punakha town (n= 272) and Paro town
465 (n=262). The greatest road (roads, footpaths, tracks) inundation occurs in Chhoekhor, followed
466 by Lunana and Saephu, while most farmland is impacted in LGUs such as Bumthang town
467 (2.3 km²), Dzomi Gewog (1.2 km²) and Paro town (1.1 km²) (Table S2).

468 **4.3 Potentially dangerous glacial lakes**

469 We defined glacial lake danger in Bhutan based on the total damage associated with each
470 lake. Of the total lakes studied here (278), 164 had zero damage index as the GLOF from
471 these lakes does not impact any buildings. Among other lakes, with the highest D_g , Thorthormi
472 Tsho in the Punatsangchu basin emerged as the very high PDGL in Bhutan (Fig. 3). Five
473 other lakes are identified as high PDGL, which are distributed across the Wangchu (2),
474 Chamkharchu (2), and Punatsangchu (1) basins. Twenty-two of the glacial lakes were in the
475 moderate danger category: seven in Punatsangchu, four in Drangmechu basin, three in
476 Chamkharchu, two in Kurichu and one in Wangchu basins (Fig. 3). The remaining (250) were
477 classified as low danger. None of the high or very high danger glacial lakes were located within
478 the Chinese and Indian sides of the basins, which drain into Bhutan (Fig. 3).



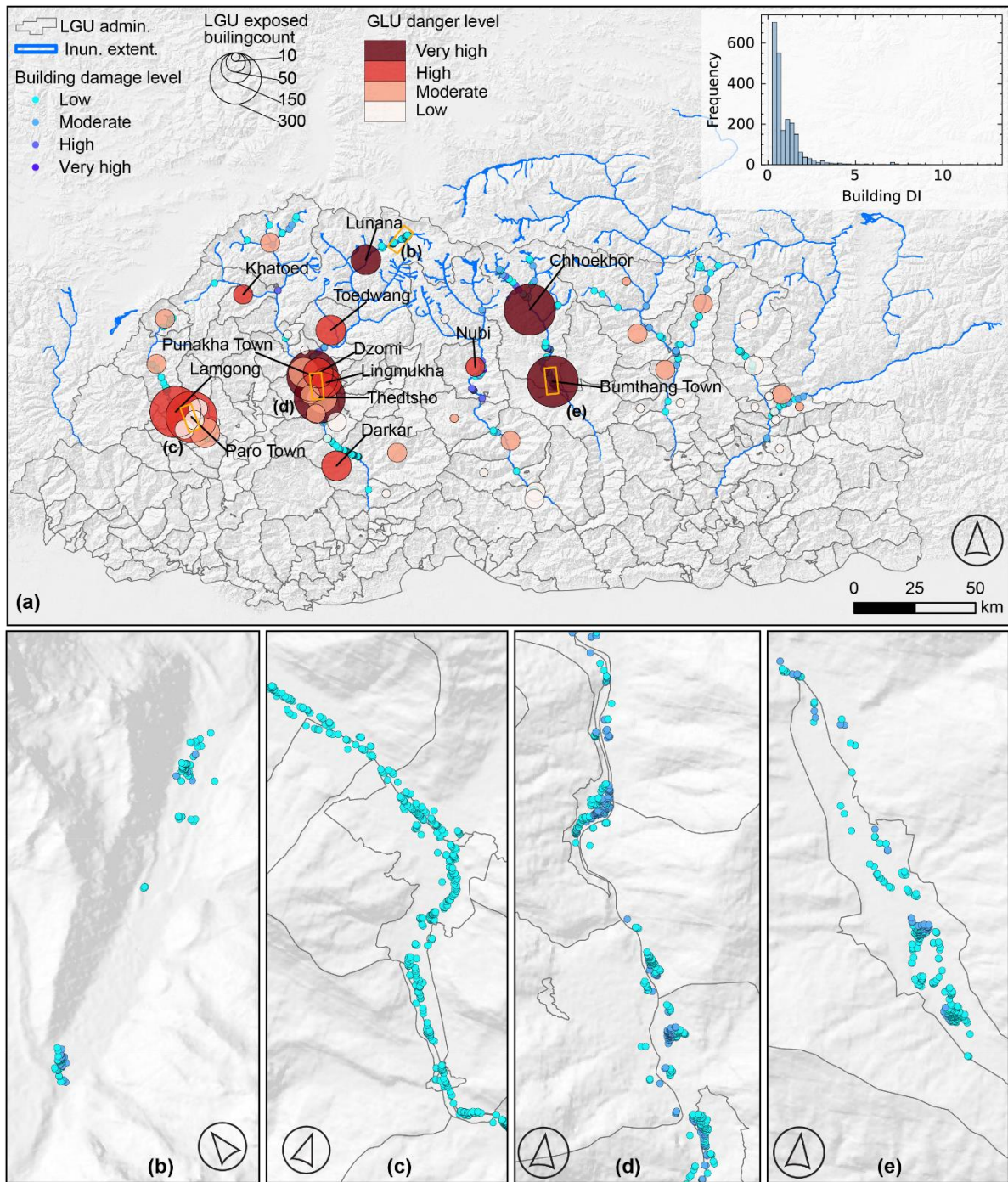
479

480 **Figure 3. Distribution of dangerous glacial lakes.** The (a) map shows the distribution of
 481 glacial lakes with associated GLOF danger levels (D. level) across the eight glaciated basins
 482 in Bhutan: very high (VH), high (H), moderate (M) and low dangers. The bar charts within the
 483 map show the number of glacial lakes (where the height of the bar corresponds to the number
 484 of lakes in each basin, referenced to the inset bar) with various danger levels in each basin.
 485 The boxes along the flood path show the number of buildings per km². The (b) bar chart shows
 486 the damage index (normalized between 0 to 1) associated with the top 20 lakes arranged in
 487 ascending order (left to right). The lake ID on the x-tick label correspond to the ID on the map.

488 4.4 Downstream GLOF danger

489 In this section, we present the GLOF danger ranking and level associated with downstream
 490 communities, encompassing 20 districts and 274 LGUs. Based on the damage index for

491 respective LGUs, which accounts for both damage from GLOF and people's vulnerability (Fig.
 492 S5), Punakha is identified as the district that would suffer from the highest GLOF damage in
 493 the future, followed by Bumthang and Wangdue Phodrang districts.



494
 495 **Figure 4. Downstream GLOF danger.** GLOF danger level across (a) LGUs and GLOF
 496 inundation extent (innun. extent). Inset bar graph in (a) shows the number of buildings in
 497 Bhutan impacted by the modelled GLOF and associated damage level: very high (VH), high

498 (H), moderate (M) and low (L). The lower panels (c–f) are the zoomed-in maps from panel (a)
499 which shows the damage level associated with individual buildings.

500 Among the LGUs, five of them were classified as having very high GLOF danger, including:
501 Chhoekhor, Punakha town, Lunana, Thedtsho, and Bumthang town (Fig. 4). Further, eight
502 others were associated with high GLOF danger. Likewise, 18 LGUs were associated with
503 moderate GLOF danger, while the rest were identified as low danger LGUs (Fig. 4).

504 **4.5 Flow arrival time**

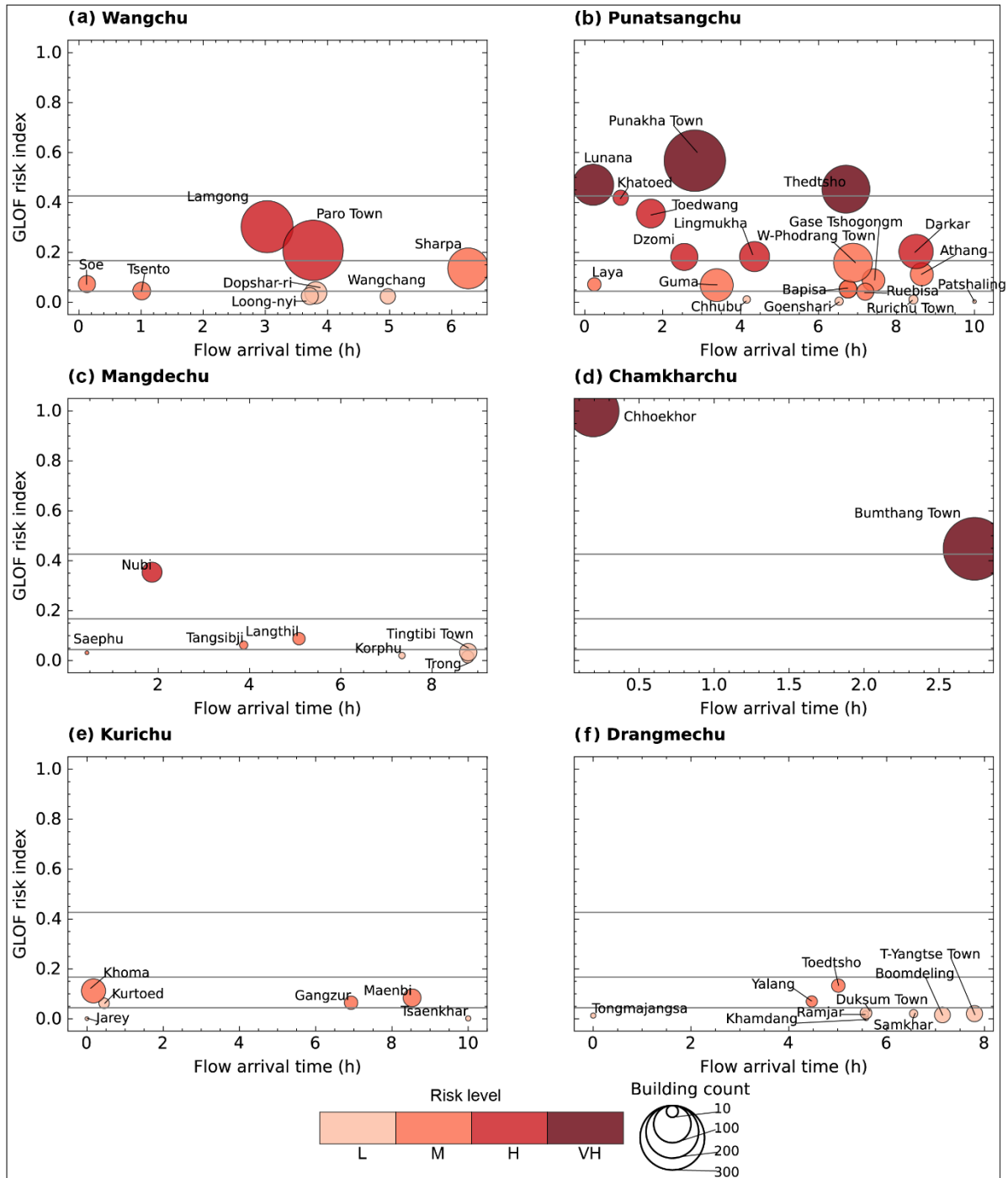
505 We also ranked the LGUs based on the flow arrival time of the GLOF scenario that would
506 impact the first buildings in the LGU. Results showed that, for the seven gewogs including
507 Soe, Khoma, Chhoekhor, Lunana, Laya, Saephu, and Kurtoed, the fastest GLOF can impact
508 some of their buildings within 30 minutes. Some buildings in Khatoed, Tsentso, Toedwang and
509 Nubi could be affected within one hour. Nine gewogs can be affected within 2 to 4 hours,
510 another nine within 4-6 hours, while the fastest GLOF could take more than 6 hours to affect
511 buildings in other LGUs (Fig. 5).

512 In the LGUs such as Soe and Laya, the first buildings affected by the GLOF are typically
513 isolated and located very close to glacial lakes. Despite their proximity, the GLOF danger
514 ranking for these LGUs remains relatively low due to the limited number of exposed buildings
515 in these LGUs (Fig. 5). Therefore, we compared the Di and the arrival time of the fastest-
516 arriving GLOF within each LGU. This analysis identified Lunana and Chhoekhor as LGUs with
517 very high GLOF danger levels, and the fastest GLOF can arrive in as little as 15 minutes. On
518 the other hand, the fastest GLOF impacting buildings takes up to three hours for other LGUs
519 with very high GLOF danger, such as Punakha town and Bumthang town (Fig. 5).

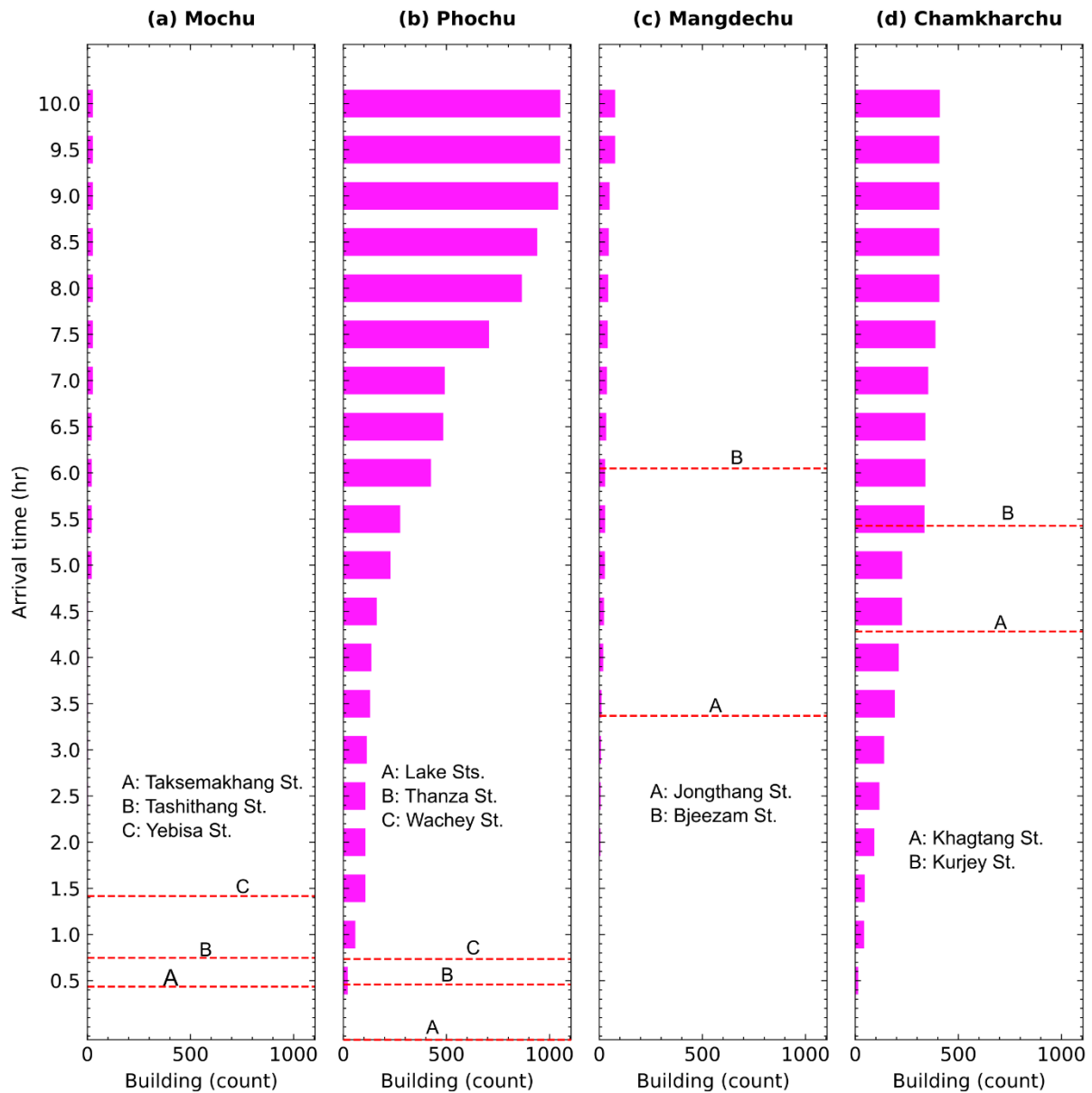
520 **4.6 Early Warning System and GLOF**

521 We analyzed the distribution of the existing GLOF early warning system in Bhutan with respect
522 to PDGLs and downstream communities associated with GLOF danger. Currently, Bhutan has
523 a GLOF early warning system in three basins: Punatsangchu, Mangdechu, and Chamkharchu.
524 Across these basins, the system is equipped with 13 monitoring stations placed at various
525 locations (Fig.1). Assuming that GLOFs from a lake may be monitored if an EWS monitoring
526 station is located downstream of the glacial lake, our study shows that the existing EWS
527 currently tracks 51 out of the 278 glacial lakes we investigated here. Among these monitored
528 lakes, the network includes the most dangerous glacial lake, Thorthormi Tsho, as well as two
529 of the five high danger glacial lakes and five of the six moderate danger glacial lakes. The
530 remaining monitored lakes are classified as low or very low danger. Notably the high danger

531 glacial lakes identified here including lake251, lake262 and lake278 are not monitored by the
 532 existing early warning systems.



533
 534 **Figure 5.** The damage index and flow arrival time of the fastest arriving GLOF for each local
 535 administrative unit (LGUs) in impacted basins: (a) Wangchu, (b) Punatsangchu, (c)
 536 Mangdechu, (d) Chamkharchu, (e) Kurichu and (f) Drangmechu. The horizontal grey lines
 537 categorize LGUs into various GLOF danger levels based on the damage index (low danger
 538 level to very high danger level).



539

540 **Figure 6.** Bar plots showing the number of buildings located downstream of GLOF early
 541 warning monitoring stations in Punatsangchu basin [(a) Mochu, (b) Phochu], (c) Mangdechu,
 542 and (d) Chamkharchu basins. Red dashed lines represent the location of EWS monitoring
 543 stations relative to the average flow arrival time of all GLOFs detected by each EWS
 544 monitoring station. The names and location of each EWS monitoring station are indicated with
 545 a letter (A to C) within the respective panel. The monitoring stations located at the lakes,
 546 including Bechung, Raphstreng, Thorthormi and Lugge Tsho in Phochu basin, are marked as
 547 “Lake Sts.” in panel (b).

548

549

550

We further examined how many residents within GLOF exposed buildings could receive early warnings based on their hydrological relationship to the existing EWS monitoring stations. Assuming that the buildings located downstream of the EWS monitoring stations can receive

551 early warning, our study revealed that the existing GLOF monitoring stations can provide early
552 warning to the people living in 1,549 buildings, of which about 75% are in the Punatsangchu
553 basin. Of these, residents in 268 buildings are estimated to have less than 30 minutes to
554 evacuate after receiving a warning from the EWS monitoring stations located in their
555 respective communities (Fig. 6).

556 Conversely, people living in 1,050 exposed buildings, that is, at least 41% of them, do not have
557 access to early warning coverage. Approximately half of these unserved buildings are
558 clustered in downstream LGUs with high GLOF danger, including Lamgong and Paro Town in
559 Paro districts. Although EWS is in place in the Chamkharchu basin, a cluster of about 82
560 buildings in Chhoekhor in Bumthang is not covered by EWS. This is because the flood waves
561 from the potential GLOF can arrive at these buildings before activating the monitoring stations
562 at Khagtang and Kurjey (Fig. 6).

563 **4.7 Sensitivity analysis**

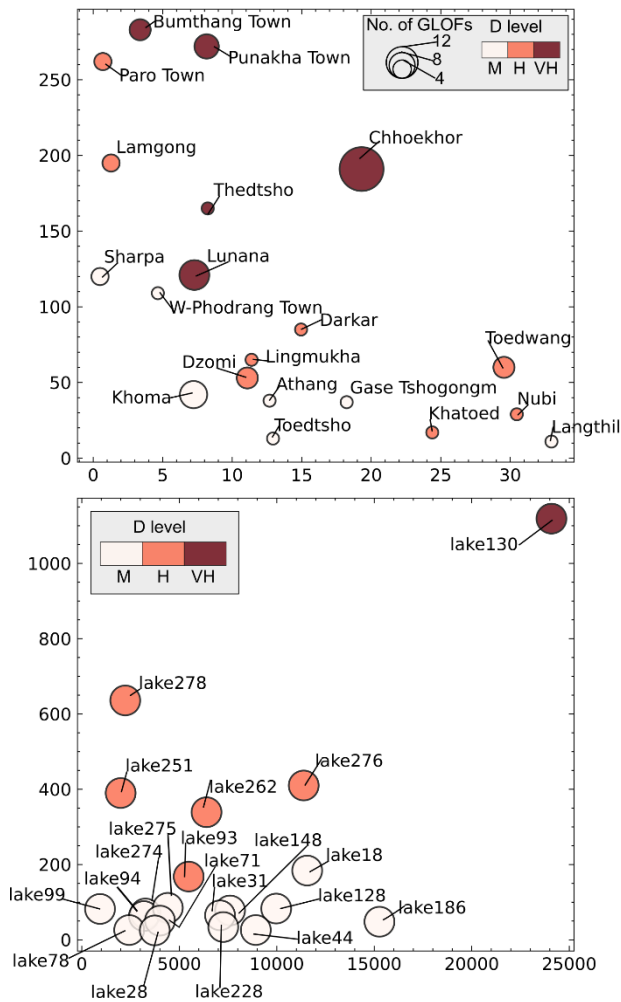
564 The sensitivity analysis revealed that the mean DV increases proportionately in response to
565 the increased in lake area. For example, when the area of lake increased by 2 orders of
566 magnitude (0.01 to 5 km) the resulting DV also increases by the same order of magnitude.
567 The variation of Manning's roughness coefficient (n) between 0.04 and 0.07 results to linear
568 increase DV ($R^2 > 0.88$) across all area categories (0.01, 0.05, 0.1, 1, and 5 km²). To evaluate
569 how lake size modulates this sensitivity, we compared the slope (β_1) of all regression
570 equations, which represents the expected change in DV for one unit increase in n . The result
571 indicates that the influence of n on DV becomes progressively more pronounced with
572 increasing lake area. Specifically, when the area was increased from 0.01 to 5 km² the value
573 of β_1 increased by one order of magnitude: from 1.23 to 58.7 m² s⁻¹. Intermediate values show
574 a consistent upward trend: $\beta_1 = 4.7$ m² s⁻¹ at 0.05 km² and 48.7 m² s⁻¹ at 1 km², indicating that
575 larger lakes amplify the hydraulic sensitivity to roughness variations (Fig. S6).

576 **5 Discussion**

577 **5.1 Redefined potentially dangerous glacial lake**

578 Some of the most damaging historical GLOF events in the world have occurred from
579 seemingly inconspicuous glacial lakes (Allen et al., 2015; Petrakov et al., 2020), whilst some
580 large-magnitude GLOF events have caused minimal or no downstream damage (Shrestha et
581 al., 2023; Lützow et al., 2023). This is because the GLOF magnitude alone does not determine
582 downstream damage caused by the GLOF event; instead, it is the interaction between GLOF
583 magnitude and the downstream exposed elements that determines the extent of damage
584 (Taylor et al., 2023a). For example, the greatest structural damage associated with the 2023

585 South Lhoknak Lake GLOF event in the Indian state of Sikkim occurred between 200 and 385
 586 km downstream of the glacial lake, with 59% of these impacted structures constructed within
 587 the past decade (Sattar et al., 2025b). This highlights the escalating exposure and so the risk
 588 due to infrastructure expansion and settlement growth in GLOF-exposed areas (Nie et al.,
 589 2023) and underscores the importance of considering exposure data in GLOF danger
 590 assessment. To address this in Bhutan, we redefined potentially dangerous glacial lakes by
 591 coupling flood characteristic modelling and downstream exposure data. Accordingly, we have
 592 produced flood mapping and GLOF danger ranking for 278 glacial lakes, along with
 593 comprehensive GLOF danger assessments for 274 local government administrative units
 594 (LGUs). As a result, we classified lake130 (Thorthormi Tsho) as a very high danger glacial lake
 595 in Bhutan, five lakes (lake93, lake251, lake262, lake276 and lake278) as high danger and 20
 596 other lakes as moderate danger. Likewise, five downstream LGUs were associated with very
 597 high GLOF danger, while eight others were associated with high GLOF danger.



598

599 **Figure 7.** Dot plot illustrating the influence of GLOF magnitude and downstream exposure on
 600 danger level computed in this study for (a) downstream LGUs and (b) individual lakes. In panel

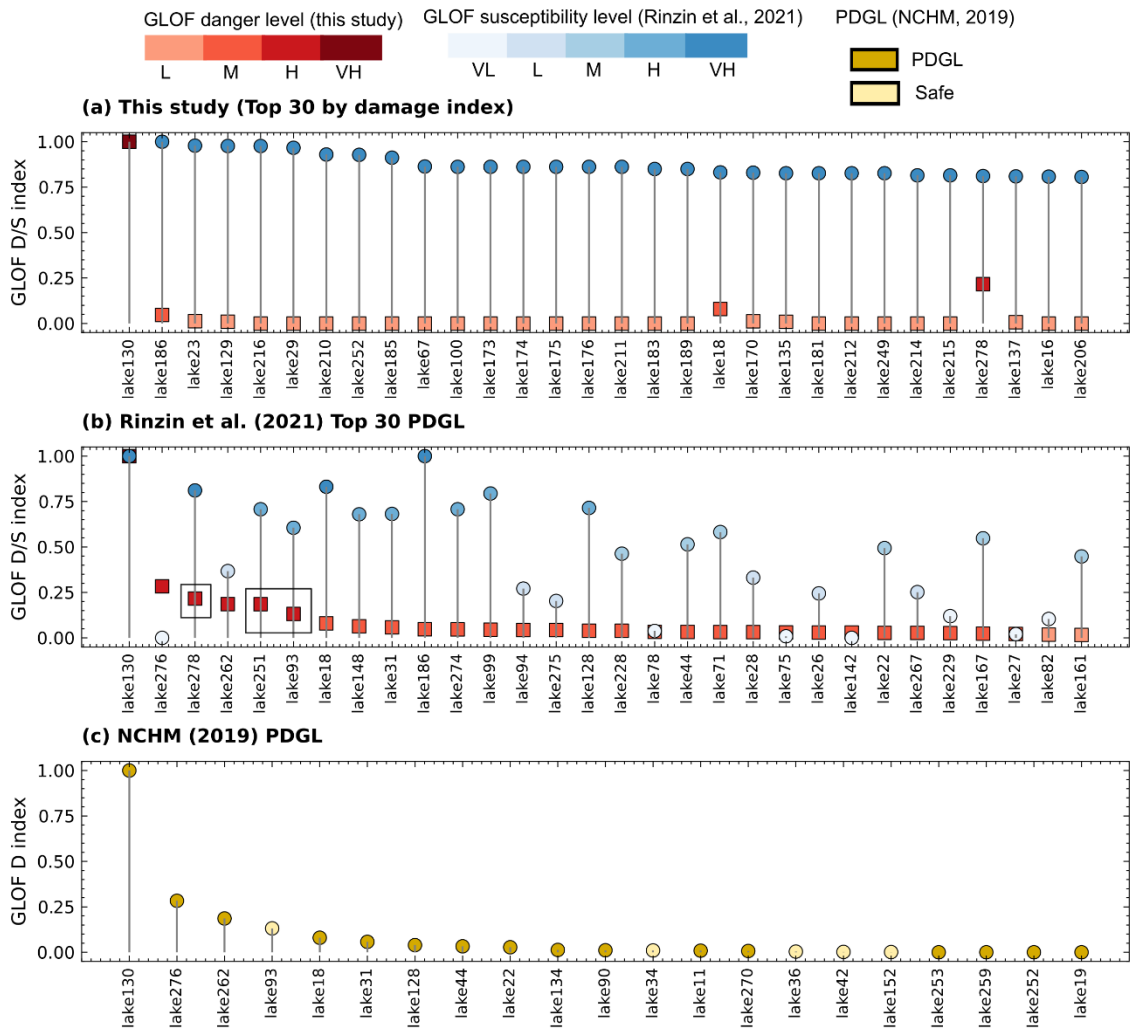
601 (a), the GLOF magnitude is based on median depth-velocity across all the GLOFs that strike
602 at least one building in the LGU. In panel (b), we considered peak discharge (Q_p) as a proxy
603 for GLOF magnitude. In both panels, the colour associated with each dot indicates the GLOF
604 danger (d) level associated with each LGU or lake. The size of the dots in panel (a)
605 corresponds to the number of GLOFs from various glacial lakes that impact the respective
606 community. For better visualization, only the top 15 PDGLs and the top 15 LGUs with GLOF
607 danger are displayed here.

608 Our approach departs from many existing practices of identifying dangerous glacial lakes,
609 which are primarily based on the susceptibility of lakes to produce GLOF without regarding
610 the characteristics of settlements located downstream of the lakes (Rinzin et al., 2021; NCHM,
611 2019), in two ways: **1) Incorporation of GLOF Hydrodynamic characteristics:** we
612 considered flow velocity and flow depth, which are both primary components of the GLOF flow
613 that determine damage to the downstream elements (Federal Emergency Management
614 Agency, 2004). **2) Interaction of flow depth and velocity with downstream exposed
615 buildings:** We mapped potential downstream building damage associated with each GLOF
616 event based on the interaction between the depth-velocity and downstream at risk elements.
617 By focusing on the interaction between flood magnitude and downstream exposed buildings,
618 our method classifies glacial lakes as dangerous only when their potential flood poses a threat
619 to downstream elements, making it a more practical and effective strategy for bespoke GLOF
620 risk reduction activities. For example, lake278 and lake251 are small, and they produce
621 relatively small GLOFs with their estimated peak discharge approximately $2000 \text{ m}^3 \text{ s}^{-1}$.
622 However, both were classified as high danger as the GLOF from these lakes impacts hundreds
623 of downstream buildings (Fig. 7). Likewise, our approach assigns a higher GLOF danger
624 ranking to communities that are either affected by GLOFs from multiple lakes, impacted by
625 high-magnitude GLOFs, or have multiple buildings located within the GLOF inundation area,
626 whilst also considering the community's vulnerability. For example, Chhoekhor was identified
627 as having the highest GLOF danger in Bhutan because at least 191 buildings were potentially
628 impacted by GLOF from as many as 14 lakes in the basin. On the other hand, gewogs such
629 as Toedwang in Punakha are also classified as having very high GLOF danger, despite having
630 a comparatively low number (60) of potentially impacted buildings, because these buildings
631 could be impacted by very high magnitude GLOFs in terms of depth and velocity (Fig. 7).

632 We classified only one lake (Thorthormi Tsho) as a very high danger glacial lake. This is
633 because, at about $\sim 4.3 \text{ km}^2$ in size, Thorthormi Tsho is the largest glacial lake, approximately
634 double the size of the next largest glacial lake in Bhutan. Moreover, Thorthormi Tsho is located
635 in the Punatsangchu basin, which is among Bhutan's most populated basins, resulting in

636 exposure of up to 1,119 buildings, again, an order of magnitude more exposure than the next
637 lake associated with the highest exposure. These findings further highlight the importance of
638 strengthening risk mitigation measures for Thorthormi Tsho and the affected downstream
639 settlements.

640 Our study complements conventional PDGL assessment approaches by redefining which
641 glacial lakes pose the greatest danger to the downstream settlements. As a result, we
642 identified three new high danger glacial lakes, including lake93 (Phudung Tsho), lake251, and
643 lake278 (Wonney Tsho), which are not recognized as PDGL by any of the previous studies.
644 Also, 53 of the previously identified 64 very highly susceptible to GLOFs lakes (Rinzin et al.,
645 2021) are categorized as low GLOF danger lakes. Conversely, 12 lakes classified as low or
646 very low GLOF susceptibility emerge as moderate to high danger in our study (Rinzin et al.,
647 2021). Likewise, nine of the dangerous lakes monitored by NCHM (six in Punatsangchu basin,
648 one each in Mangdechu, Chamkharchu and Kurichu basins) (NCHM, 2019) are categorized
649 as low danger in our study (Fig. 8). These discrepancies arise because we classified lakes as
650 dangerous only if a potential GLOF would affect a significant number of downstream buildings,
651 whereas earlier studies' definitions are motivated by the likelihood of producing GLOF based
652 on characteristics of lake and surrounding terrains (Rinzin et al., 2021; NCHM, 2019) (Fig. 8).
653 For example, lake278 in the Wangchu headwaters is classified as high danger in our study
654 because a potential GLOF could impact 636 buildings across seven LGUs in Paro while the
655 earlier studies considered this lake as safe as it does not have geomorphological
656 characteristics and lake condition to qualify as dangerous (Rinzin et al., 2021).



657

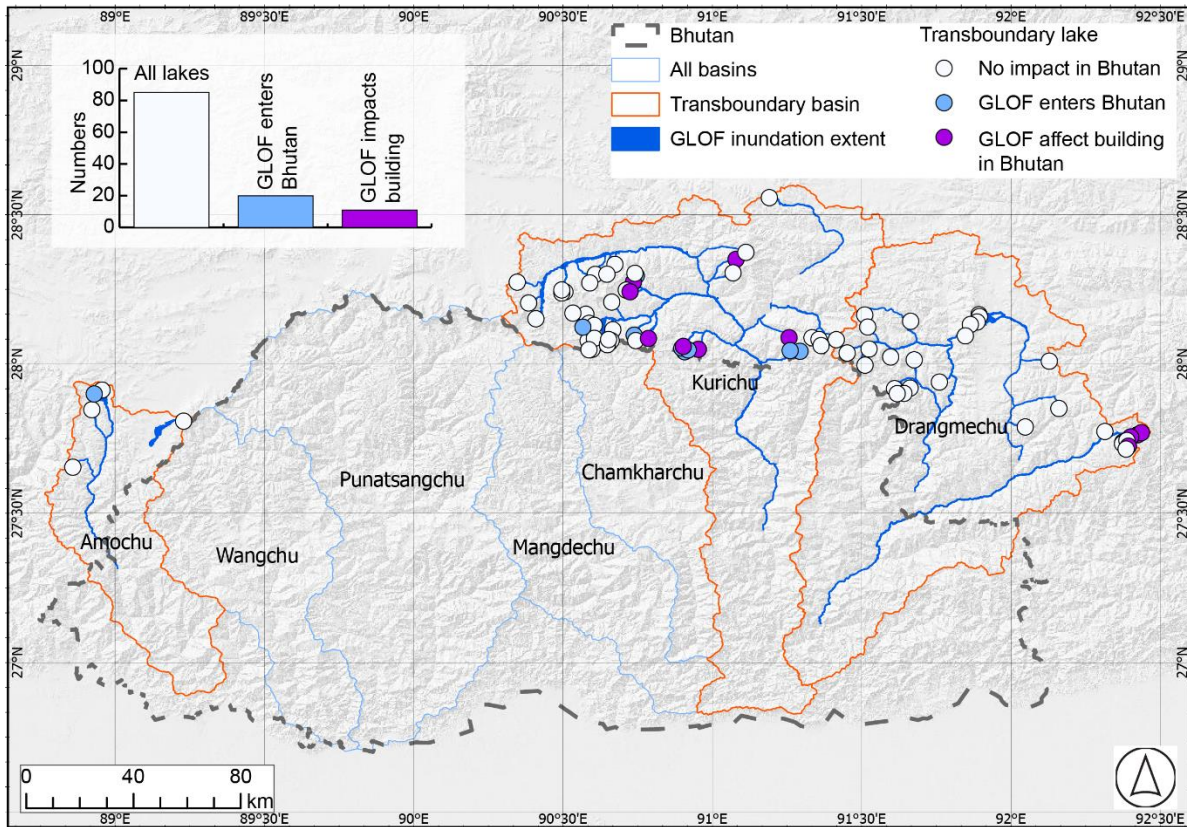
658 **Figure 8.** Comparison (a, b) GLOF damage index (DI) for the top 30 PDGL calculated in the
 659 current study and GLOF susceptibility score from Rinzin et al. (2021), and (c) damage index
 660 (DI) for PDGLs in Bhutan identified by the NCHM (2019). The black bounding box in panel (b)
 661 shows the new PDGLs identified in this study for the first time.

662 By ranking GLOF danger for all 274 LGUs, we discovered a potential new GLOF risk hotspot,
 663 such as Paro town and Lamgong gewog in Paro and Chhoekhor gewog in Bumthang. GLOF
 664 danger in these places was previously not quantified, and existing GLOF early warning
 665 systems in Bhutan currently do not cover these high GLOF danger LGUs (NCHM, 2021). We
 666 therefore recommend prioritizing monitoring of glacial lakes in Bhutan based on all
 667 components of risk (hazard, exposure and vulnerability), rather than focusing on lakes
 668 selected solely based on geomorphic susceptibility assessments, which takes care of only the
 669 likelihood of producing GLOF. Specifically, Bhutan's glacial lake monitoring and downstream
 670 risk mitigation efforts should expand beyond Lunana to include other high GLOF danger lakes
 671 and vulnerable downstream settlements such as Paro Town and Chhoekhor gewog, while

672 emphasising that higher granularity studies might be needed to guide bespoke risk reduction
673 efforts in these respective areas.

674 **5.2 Transboundary GLOF**

675 None of the transboundary lakes were classified as very high or high danger based on
676 potential GLOF impacts in Bhutan. This is because damage was minimal, mainly inundating
677 uninhabited parts of Bhutan, located in deep, inaccessible gorges. However, we identified
678 GLOF from four lakes in the Drangmechu basin (located in Arunachal Pradesh, India) and 11
679 in the Kurichu basin (located in the Tibetan Autonomous Region, China), which could
680 potentially impact several buildings in Bhutan. Furthermore, GLOF from 20 lakes located in
681 the Indian and Chinese territories of the Himalaya enter Bhutan, although they do not impact
682 any building (Fig. 9). The modelled GLOF from all lakes in Bhutan attenuates before it crosses
683 the international border between Bhutan and India. However, we acknowledge that some of
684 the GLOF events in the future can impact settlements along transboundary river floodplains
685 in India, especially under the worst-case scenarios and when their flows are amplified by the
686 addition of material along the flow path, such as from a landslide deposit (Cook et al., 2018)
687 and hydropower dam (Sattar et al., 2025b). Identifying potential transboundary GLOFs is vital,
688 given their potential destructive power and long run out distances and challenges stemming
689 from the absence of transboundary GLOF risk mitigation mechanisms. For example, a recent
690 GLOF from South Lhoknak Lake in the Indian Himalaya has travelled over 300 km
691 downstream, causing significant damage in Bangladesh (Sattar et al., 2025b). The absence
692 of transboundary cooperation for GLOF risk mitigation between Bhutan, China, and India
693 complicates efforts to monitor and manage such risks. Establishing regional cooperation is
694 essential to enhance early warning systems, facilitate data sharing, and implement
695 coordinated risk reduction strategies such as one proposed by Zhang et al. (2025), thereby
696 minimizing the potential damage from future transboundary GLOFs.



697

698 **Figure 9.** The map shows the impact of GLOF in Bhutan, which originates from lakes located
 699 on the Chinese and Indian sides of transboundary basins. The inset bar graph shows the total
 700 lakes, lakes from which GLOFs enter Bhutan and lakes from which GLOF impacts buildings
 701 in Bhutan. The lake ID on the x-tick labels corresponds to the ID on the map.

702 **5.3 Significance, limitations and the way forward**

703 **5.3.1 Significance**

704 Our approach of GLOF danger assessment using both flood magnitude and downstream
 705 exposure data provides local authorities and relevant stakeholders with valuable information
 706 to plan and prioritize wide-ranging risk mitigation activities. These activities may target either
 707 specific glacial lakes or downstream communities based on the damage index and level we
 708 have provided, whilst also incorporating practical factors, such as resource availability and
 709 logistical constraints. This study is particularly timely, as the Royal Government of Bhutan is
 710 planning to modernize and expand its network of flood monitoring and GLOF early warning
 711 systems (World Bank, 2024). This initiative, outlined in the roadmap for 2024–2034, aims to
 712 develop multi-hazard warning services, aligning closely with the practical applications and
 713 insights provided by our research. For example, our flood mapping and flow arrival time data
 714 can be used to appropriately locate GLOF monitoring stations for early warning systems
 715 (Wang et al., 2022). Likewise, some of the scattered buildings in LGUs such as Soe gewog in

716 Paro could be impacted by GLOFs within as little as 10 minutes. This short lead time means
717 it is practically not effective to install early warning systems for residents in these rapidly
718 affected areas. In such context, our flood extent mapping can effectively guide land-use zoning
719 and support targeted decision-making for future development in these vulnerable locations.

720 **5.3.2 Limitations and the way forward**

721 Our work establishes a baseline GLOF mapping and risk assessment in Bhutan. However, we
722 acknowledge that the magnitude of flood from glacial lakes will continue to evolve as glacier
723 retreat drives the expansion of existing lakes within a topographically constrained extent and
724 the formation of new lakes within the depressions left by the retreating glaciers (Zheng et al.,
725 2021b; Furian et al., 2022). This increasing lake area is expected to amplify GLOF magnitude
726 in terms of hydraulic intensity, as supported by our sensitivity analysis, which shows that the
727 that DV increases approximately by two orders of magnitude when area increases from 0.01
728 to 5 km². Concomitantly, the downstream settlements within the GLOF-prone areas are
729 evolving, with population growth and infrastructure development leading to increased GLOF
730 exposure. The interplay of these factors means GLOF danger will likely increase in the future
731 and highlights the need for dynamic and regularly updated GLOF flood mapping and risk
732 assessments in the future.

733 We determined the minimum glacial lake area threshold (0.05 km²) for GLOF modelling based
734 on the empirical evidence from the previous inventory (Shrestha et al., 2023; Komori et al.,
735 2012). However, it is important to acknowledge that glacial lakes smaller than 0.05 km² have
736 also been known to produce GLOFs with a magnitude substantial enough to cause significant
737 downstream damage (Sattar et al., 2025a), particularly when they combine with other floods
738 like meteorological flood (Allen et al., 2015) or when the outburst flow entrains large amount
739 of debris (Petrakov et al., 2020; Cook et al., 2018). Thus, the future modelling efforts should
740 also consider smaller lakes than the size threshold we considered here.

741 Our drainage volume and peak discharge calculations are based on empirical equations and
742 the previous GLOF events, with scarcely documented detailed characteristics (Shrestha et al.,
743 2023). Employing such proxy parameters is reasonable for this study as we aimed to provide
744 an overview of GLOF danger in Bhutan based on the downstream impact. The modelled GLOF
745 scenarios for each lake are directly comparable, enabling an assessment of the overall and
746 relative levels of danger, and representing a moderate scenario. We recognize, however, that
747 this is just one set of scenarios while empirical relationship between the volume and area are
748 associated with significant uncertainty (Schwanghart et al., 2016). Due to time and
749 computational constraints, it was not feasible to simulate all potential variations. Future studies
750 focusing on the detailed impact of specific glacial lakes or on specific downstream

751 communities must be grounded on site-specific scenario informed by situational triggering
752 factors and dam composition and geometry. The study should also consider the site-specific
753 worst-case scenario, considering the future climatic conditions.

754 While we mapped all types of exposed elements located within the GLOF flow inundation
755 extent, our GLOF damage index is calculated solely based on the impact on the number of
756 exposed buildings. This approach is grounded in the rationale that buildings represent the
757 primary places where people reside and are therefore the most direct proxy for population
758 exposure. However, critical infrastructure such as hydropower plants (e.g., in the
759 Punatsangchu basin) and the international airport in Paro (Wangchu basin), which are vital to
760 the national economy, were not included in our danger calculation. This omission stems from
761 the considerable challenges involved in accurately estimating the economic cost of potential
762 damage to such high-value infrastructure. When the GLOF intercepts hydropower dams, it
763 can cause overtopping, excessive sedimentation, outages, and equipment damage, leading
764 to significant revenue losses from the hydropower plants (Dunning et al., 2006) as well as
765 cascading impacts on the low-lying settlements (Sattar et al., 2025b). Likewise, damage to the
766 crucial infrastructure, such as Paro international airport, will hinder relief efforts after the GLOF
767 disaster, delaying the recovery and escalating overall loss and damage. Therefore, future
768 studies should also consider absolute economic impact of GLOF to aid relevant stakeholders
769 and policymakers in developing appropriate strategies to mitigate risks to vital infrastructure.

770 The socio-economic indicators used here are the best available census data at the finest
771 granularity in Bhutan. These indicators represent people's capability to respond to and recover
772 from not only GLOF but also any natural or man-made hazards (Cutter et al., 2003). However,
773 these indicators do not necessarily represent people's specific vulnerability to GLOF, as it also
774 depends on other factors such as prior experience of natural hazards (Lloyd's Register
775 Foundation, 2024). For example, we classified Lunana gewog as the most vulnerable gewog
776 based on these socio-economic indicators (Fig S5); however, how their prior experience
777 influences their response capability remains beyond the scope of this study. Future studies
778 focusing on specific downstream settlements or impact of a particular glacial lake should also
779 consider the broader implications of vulnerability and resilience.

780 Looking forward, the glacial lake dataset can be updated using wide-ranging open-access
781 remote sensing imagery. Similarly, platforms such as OpenStreetMap, which leverage
782 crowdsourced data and are frequently updated, present a valuable resource for mapping
783 evolving downstream buildings and other structure data. Likewise, hydrodynamic modelling
784 for multiple glacial lakes with freely available and user-friendly models such as HEC-RAS is
785 increasingly becoming feasible with the recent development in artificial intelligence and cloud-

786 based computing platforms like Flood Platform (<https://www.floodplatform.com/>), which enable
787 integrating products from varied flood simulations/models into a common framework. We have
788 developed a website, which hosts glacial lake data and flood maps, serving as a valuable
789 resource for periodic updates to flood damage assessments. By integrating up-to-date glacial
790 lake flood magnitude information with evolving downstream exposure data, this platform can
791 provide valuable information for informed decision-making and proactive risk management,
792 such as tailored early warning systems and land use management and development.

793 **6 Conclusion**

794 Glacial lakes, which are growing in number and area in mountains globally, pose a serious
795 GLOF threat to the communities living downstream of them. However, the destruction and
796 damage caused during the GLOF event are not determined solely by flood magnitude or
797 intensity, but also depend on their interaction with downstream exposed elements. Despite
798 this, traditional approaches to assessing the danger posed by glacial lakes have been mainly
799 based on the likelihood and magnitude of a lake to produce GLOF and often disregard the
800 potential downstream impact. To address this gap, this study redefines the classification of
801 PDGLs in Bhutan (one of the high GLOF risk countries globally) by combining GLOF
802 hydrodynamic characteristics and downstream exposed buildings.

803 This study produced GLOF hydrodynamic characteristics for all glacial lakes in Bhutan that
804 are greater than 0.05 km² and located within 1 km of a glacier terminus. The analysis revealed
805 that over 11,322 people, 2,600 buildings, as well as other infrastructure such as roads, bridges
806 and farmland are exposed to GLOF in Bhutan. A GLOF damage index was developed by
807 combining flood mapping data with downstream exposure metrics, enabling the ranking of
808 glacial lakes based on their potential danger. Thorthormi Tsho was identified as the most
809 dangerous glacial lake in Bhutan. Furthermore, we identified five additional glacial lakes as
810 having high GLOF danger, two of which are in the headwaters of Wangchu, neither included
811 in the previous study nor monitored by the existing early warning system in Bhutan. Among
812 these dangerous glacial lakes, three of them are newly identified potentially dangerous glacial
813 lakes (lake251, 278 and lake93) in the current study.

814 For the first time, this study provides GLOF danger ranking for 20 districts and 274 local
815 government administrative blocks (gewogs and towns) [LGUs] in Bhutan. In addition to the
816 previously identified high GLOF danger gewogs and towns, we have identified six additional
817 LGUs with similarly high GLOF dangers. These include Chhoekhor and Bumthang town in
818 Bumthang, Paro town and Lamgong in Paro, Nubi in Trongsa and Khoma in Lhuentse districts.
819 Most strikingly, some downstream LGUs such as Paro town and Lamgong gewog in Paro are

820 not covered by the existing Bhutan early warning system, highlighting significant gaps in
821 existing risk mitigation efforts.

822 This study underscores the criticality of incorporating flood mapping and downstream
823 exposure and vulnerability data when defining PDGLs and assessing downstream risk. For
824 Bhutan, the findings emphasize the urgent need to expand and strengthen GLOF risk
825 mitigation strategies, including the enhancement of early warning systems and the
826 implementation of targeted interventions in newly identified high-risk areas. These measures
827 are essential to safeguarding vulnerable communities and infrastructure from the escalating
828 threat of GLOFs in the context of ongoing climate change and glacial retreat.

829 **7 Acknowledgement**

830 This work was supported by the Natural Environment Research Council (NERC)- funded
831 IAPETUS Doctoral Training Partnership [IAP2-21-267].

832 **Code and data availability**

833 The HEC-RAS 2D model we used here for simulating glacial lake outburst modelling can be
834 accessed at: <https://www.hec.usace.army.mil/>. The AW3D30 DEMS used here can be
835 downloaded from the OpenTopography at: [OpenTopography - Find Topography Data](#). Bhutan
836 2017 housing and census data can be downloaded from National Statistical Bureau of Bhutan
837 at <https://www.nsb.gov.bt/>. Landcover and landuse data used in this study can be accessed at:
838 <https://rds.icimod.org/>. The OpenStreetMap data can be assessed at:
839 <https://www.openstreetmap.org/relation/184629>. GLOF hydraulic data for each glacial lake will
840 be made available through web portal upon publication of this article.

841 **Supplement**

842 The supplement related to this article is available online at:

843 **Author contributions**

844 SR, SD and RC conceptualized the study. SR undertook data analysis, visualization and wrote
845 original draft. SD and RC secured the funding, supervised and contributed equally to the work.
846 SA, AS and SW reviewed and edited the manuscript. All authors contributed to the final
847 manuscript.

848 **Competing interests**

849 The contact author has declared that none of the authors has any competing interests.

850

851 **References**

- 852 Allen, S., Frey, H., and Huggel, C.: Assessment of Glacier and Permafrost Hazards in Mountain Regions.
 853 Technical Guidance Document, 10.13140/RG.2.2.26332.90245, 2017.
- 854 Allen, S. K., Rastner, P., Arora, M., Huggel, C., and Stoffel, M.: Lake outburst and debris flow disaster at
 855 Kedarnath, June 2013: hydrometeorological triggering and topographic predisposition, *Landslides*, 13,
 856 1479-1491, 10.1007/s10346-015-0584-3, 2015.
- 857 Allen, S. K., Zhang, G., Wang, W., Yao, T., and Bolch, T.: Potentially dangerous glacial lakes across the
 858 Tibetan Plateau revealed using a large-scale automated assessment approach, *Science Bulletin*, 64,
 859 435-445, 10.1016/j.scib.2019.03.011, 2019.
- 860 Allen, S. K., Linsbauer, A., Randhawa, S. S., Huggel, C., Rana, P., and Kumari, A.: Glacial lake outburst
 861 flood risk in Himachal Pradesh, India: an integrative and anticipatory approach considering current and
 862 future threats, *Natural Hazards*, 84, 1741-1763, 10.1007/s11069-016-2511-x, 2016.
- 863 Byers, A. C., Rounce, D. R., Shugar, D. H., Lala, J. M., Byers, E. A., and Regmi, D.: A rockfall-induced
 864 glacial lake outburst flood, Upper Barun Valley, Nepal, *Landslides*, 16, 533-549, 10.1007/s10346-018-
 865 1079-9, 2018.
- 866 Carr, J. R., Barrett, A., Rinzin, S., and Taylor, C.: Step-change in supraglacial pond area on Tshojo Glacier,
 867 Bhutan, and potential downstream inundation patterns due to pond drainage events, *Journal of*
 868 *Glaciology*, 1-40, 10.1017/jog.2024.62, 2024.
- 869 Carrivick, J. L. and Tweed, F. S.: A global assessment of the societal impacts of glacier outburst floods,
 870 *Global and Planetary Change*, 144, 1-16, 10.1016/j.gloplacha.2016.07.001, 2016.
- 871 Chow, V. T.: *Open-channel Hydraulics*, **MacGraw-Hill Book Co**, Newyork1959.
- 872 Clausen, L. and Clark, P.: The development of criteria for predicting dambreak flood damages using
 873 modelling of historical dam failures, *International conference on river flood hydraulics*, 369-380,
 874 Colavitto, B., Allen, S., Winocur, D., Dussailant, A., Guillet, S., Munoz-Torrero Manchado, A., Gorsic, S.,
 875 and Stoffel, M.: A glacial lake outburst floods hazard assessment in the Patagonian Andes combining
 876 inventory data and case-studies, *Sci Total Environ*, 916, 169703, 10.1016/j.scitotenv.2023.169703,
 877 2024.
- 878 Cook, K. L., Andermann, C., Gimbert, F., Adhikari, B. R., and Hovius, N.: Glacial lake outburst floods as
 879 drivers of fluvial erosion in the Himalaya, *Science*, 362, 53-57, doi:10.1126/science.aat4981, 2018.
- 880 Cook, S. J., Kougkoulos, I., Edwards, L. A., Dortch, J., and Hoffmann, D.: Glacier change and glacial lake
 881 outburst flood risk in the Bolivian Andes, *The Cryosphere*, 10, 2399-2413, 10.5194/tc-10-2399-2016,
 882 2016.
- 883 Cutter, S. L. and Finch, C.: Temporal and spatial changes in social vulnerability to natural hazards, 105,
 884 2301-2306, 10.1073/pnas.0710375105 %J *Proceedings of the National Academy of Sciences*, 2008.
- 885 Cutter, S. L., Boruff, B. J., and Shirley, W. L.: *Social Vulnerability to Environmental Hazards**, 84, 242-
 886 261, <https://doi.org/10.1111/1540-6237.8402002>, 2003.
- 887 Cutter, S. L., Barnes, L., Berry, M., Burton, C., Evans, E., Tate, E., and Webb, J.: A place-based model for
 888 understanding community resilience to natural disasters, *Global Environmental Change*, 18, 598-606,
 889 10.1016/j.gloenvcha.2008.07.013, 2008.
- 890 Das, S., Kar, N. S., and Bandyopadhyay, S.: Glacial lake outburst flood at Kedarnath, Indian Himalaya: a
 891 study using digital elevation models and satellite images, *Natural Hazards*, 77, 769-786,
 892 10.1007/s11069-015-1629-6, 2015.
- 893 Dunning, S. A., Rosser, N. J., Petley, D. N., and Massey, C. R.: Formation and failure of the Tsatichhu
 894 landslide dam, Bhutan, *Landslides*, 3, 107-113, 10.1007/s10346-005-0032-x, 2006.
- 895 Emmer, A.: Understanding the risk of glacial lake outburst floods in the twenty-first century, *Nature*
 896 *Water*, 2, 608-610, <https://doi.org/10.1038/s44221-024-00254-1>, 2024.
- 897 Evans, S. G.: The maximum discharge of outburst floods caused by the breaching of man-made and
 898 natural dams, *Canadian Geotechnical Journal*, 23, 385-387, 10.1139/t86-053, 1986.
- 899 Federal Emergency Management Agency, F.: *Direct physical damage—general building stock*, HAZUS-
 900 MH Technical manual, chapter5, Federal Emergency Management Agency Washington, DC2004.

901 Furian, W., Maussion, F., and Schneider, C.: Projected 21st-Century Glacial Lake Evolution in High
902 Mountain Asia, *Frontiers in Earth Science*, 10, 10.3389/feart.2022.821798, 2022.

903 Hugonnet, R., McNabb, R., Berthier, E., Menounos, B., Nuth, C., Girod, L., Farinotti, D., Huss, M.,
904 Dussaillant, I., Brun, F., and Kaab, A.: Accelerated global glacier mass loss in the early twenty-first
905 century, *Nature*, 592, 726-731, 10.1038/s41586-021-03436-z, 2021.

906 Japan Aerospace Exploration Agency, J.: ALOS World 3D 30 meter DEM (V3.2), OpenTopography
907 [dataset], <https://doi.org/10.5069/G94M92HB>, 2021.

908 Karra, K., Kontgis, C., Statman-Weil, Z., Mazzariello, J. C., Mathis, M., and Brumby, S. P.: Global land
909 use/land cover with Sentinel 2 and deep learning, 2021 IEEE international geoscience and remote
910 sensing symposium IGARSS, 4704-4707,

911 Komori, J., Koike, T., Yamanokuchi, T., and Tshering, P.: Glacial Lake Outburst Events in the Bhutan
912 Himalayas, *Global Environmental Research* ©2012 AIRIES, 16, 12, 2012.

913 Kropáček, J., Neckel, N., Tyrna, B., Holzer, N., Hovden, A., Gourmelen, N., Schneider, C., Buchroithner,
914 M., and Hochschild, V.: Repeated glacial lake outburst flood threatening the oldest Buddhist monastery
915 in north-western Nepal, *Natural Hazards and Earth System Sciences*, 15, 2425-2437, 10.5194/nhess-
916 15-2425-2015, 2015.

917 Liu, K., Song, C., Ke, L., Jiang, L., Pan, Y., and Ma, R.: Global open-access DEM performances in Earth's
918 most rugged region High Mountain Asia: A multi-level assessment, *Geomorphology*, 338, 16-26,
919 10.1016/j.geomorph.2019.04.012, 2019.

920 Lloyd's Register Foundation: World Risk Poll 2024 Report: Resilience in a Changing World.,
921 <https://doi.org/10.60743/CORM-H862>, 2024.

922 Lützwow, N., Veh, G., and Korup, O.: A global database of historic glacier lake outburst floods, *Earth Syst.*
923 *Sci. Data Discuss.*, 2023, 1-27, 10.5194/essd-2022-449, 2023.

924 Maurer, J. M., Schaefer, J. M., Russell, J. B., Rupper, S., Wangdi, N., Putnam, A. E., and Young, N.: Seismic
925 observations, numerical modeling, and geomorphic analysis of a glacier lake outburst flood in the
926 Himalayas, *Science Advances*, 6, eaba3645, doi:10.1126/sciadv.aba3645, 2020.

927 Ministry of Economic Affairs, M.: Bhutan Sustainable Hydropower Development Policy 2021, 2021.

928 Mool, P. K., Wangda, D., Bajracharya, S. R., Joshi, S. P., Kunzang, K., and Gurung, D. R.: <Inventory of
929 Glaciers, Glacial Lakes and Glacial Lake Outburst Floods-Bhutan.pdf>, International Centre for
930 Integrated Mountain Development (ICIMOD), Kathmandu, Nepal, 2001.

931 Nagai, H., Fujita, K., Sakai, A., Nuimura, T., and Tadono, T.: Comparison of multiple glacier inventories
932 with a new inventory derived from high-resolution ALOS imagery in the Bhutan Himalaya, *The*
933 *Cryosphere*, 10, 65-85, 10.5194/tc-10-65-2016, 2016.

934 NCHM, N.: Reassessment of Potentially Dangerous Glacial Lakes in Bhutan, NCHM, Royal Government
935 of Bhutan, National Center for Hydrology and Meteorology, Royal Government of Bhutan, PO Box:
936 2017, Thimphu, Bhutan, 54, 2019.

937 NCHM, N.: Standard operating procedure (sop) for GLOF early warning system Punakha-Wangdue
938 valley, 2021.

939 National Statistics Bureau of Bhutan: 2017 Population and housing census of Bhutan, National Statistics
940 Bureau of Bhutan, Thimphu, Bhutan, 2018.

941 Nie, Y., Liu, W., Liu, Q., Hu, X., and Westoby, M. J.: Reconstructing the Chongbaxia Tsho glacial lake
942 outburst flood in the Eastern Himalaya: Evolution, process and impacts, *Geomorphology*, 370,
943 10.1016/j.geomorph.2020.107393, 2020.

944 Nie, Y., Liu, Q., Wang, J., Zhang, Y., Sheng, Y., and Liu, S.: An inventory of historical glacial lake outburst
945 floods in the Himalayas based on remote sensing observations and geomorphological analysis,
946 *Geomorphology*, 308, 91-106, 10.1016/j.geomorph.2018.02.002, 2018.

947 Nie, Y., Pritchard, H. D., Liu, Q., Hennig, T., Wang, W., Wang, X., Liu, S., Nepal, S., Samyn, D., Hewitt, K.,
948 and Chen, X.: Glacial change and hydrological implications in the Himalaya and Karakoram, *Nature*
949 *Reviews Earth & Environment*, 2, 91-106, 10.1038/s43017-020-00124-w, 2021.

950 Nie, Y., Deng, Q., Pritchard, H. D., Carrivick, J. L., Ahmed, F., Huggel, C., Liu, L., Wang, W., Lesi, M., Wang,
951 J., Zhang, H., Zhang, B., Lü, Q., and Zhang, Y.: Glacial lake outburst floods threaten Asia's infrastructure,
952 *Science Bulletin*, 10.1016/j.scib.2023.05.035, 2023.

953 Petrakov, D. A., Chernomorets, S. S., Viskhadzhieva, K. S., Dokukin, M. D., Savernyuk, E. A., Petrov, M.
954 A., Erokhin, S. A., Tutubalina, O. V., Glazyrin, G. E., Shpuntova, A. M., and Stoffel, M.: Putting the poorly
955 documented 1998 GLOF disaster in Shakhimardan River valley (Alay Range, Kyrgyzstan/Uzbekistan)
956 into perspective, *Science of The Total Environment*, 724, 10.1016/j.scitotenv.2020.138287, 2020.

957 Petrucci, O.: The Impact of Natural Disasters: Simplified Procedures and Open Problems, in:
958 *Approaches to Managing Disaster*, edited by: John, T., IntechOpen, Rijeka, Ch. 6, 10.5772/29147, 2012.

959 Rahmani, M., Muzwagi, A., and Pumariega, A. J.: Cultural Factors in Disaster Response Among Diverse
960 Children and Youth Around the World, *Current Psychiatry Reports*, 24, 481-491, 10.1007/s11920-022-
961 01356-x, 2022.

962 Rinzin, S., Zhang, G., and Wangchuk, S.: Glacial Lake Area Change and Potential Outburst Flood Hazard
963 Assessment in the Bhutan Himalaya, *Frontiers in Earth Science*, 9, 10.3389/feart.2021.775195, 2021.

964 Rinzin, S., Dunning, S., Carr, R. J., Sattar, A., and Mergili, M.: Exploring implications of input parameter
965 uncertainties in glacial lake outburst flood (GLOF) modelling results using the modelling code r.avafLOW,
966 *Natural Hazards and Earth System Sciences*, 25, 1841-1864, 10.5194/nhess-25-1841-2025, 2025.

967 Rinzin, S., Zhang, G., Sattar, A., Wangchuk, S., Allen, S. K., Dunning, S., and Peng, M.: GLOF hazard,
968 exposure, vulnerability, and risk assessment of potentially dangerous glacial lakes in the Bhutan
969 Himalaya, *Journal of Hydrology*, 619, 10.1016/j.jhydrol.2023.129311, 2023.

970 Rupper, S., Schaefer, J. M., Burgener, L. K., Koenig, L. S., Tsering, K., and Cook, E. R.: Sensitivity and
971 response of Bhutanese glaciers to atmospheric warming, *Geophysical Research Letters*, 39, n/a-n/a,
972 10.1029/2012gl053010, 2012.

973 Sattar, A., Emmer, A., Lhazom, T., Rai, S. K., and Azam, M. F.: Flood risk from small mountain lakes,
974 *Communications Earth & Environment*, 6, 10.1038/s43247-025-02758-4, 2025a.

975 Sattar, A., Goswami, A., Kulkarni, A. V., Emmer, A., Haritashya, U. K., Allen, S., Frey, H., and Huggel, C.:
976 Future Glacial Lake Outburst Flood (GLOF) hazard of the South Lhonak Lake, Sikkim Himalaya,
977 *Geomorphology*, 388, 10.1016/j.geomorph.2021.107783, 2021.

978 Sattar, A., Allen, S., Mergili, M., Haeberli, W., Frey, H., Kulkarni, A. V., Haritashya, U. K., Huggel, C.,
979 Goswami, A., and Ramsankaran, R.: Modeling Potential Glacial Lake Outburst Flood Process Chains and
980 Effects From Artificial Lake-Level Lowering at Gepang Gath Lake, Indian Himalaya, *Journal of*
981 *Geophysical Research: Earth Surface*, 128, 10.1029/2022jf006826, 2023.

982 Sattar, A., Cook, K. L., Rai, S. K., Berthier, E., Allen, S., Rinzin, S., Van Wyk de Vries, M., Haeberli, W.,
983 Kushwaha, P., Shugar, D. H., and et al.: The Sikkim flood of October 2023: Drivers, causes and impacts
984 of a multihazard cascade, *Science*, 0, eads2659, 10.1126/science.ads2659, 2025b.

985 Schwanghart, W., Worni, R., Huggel, C., Stoffel, M., and Korup, O.: Uncertainty in the Himalayan
986 energy–water nexus: estimating regional exposure to glacial lake outburst floods, *Environmental*
987 *Research Letters*, 11, 10.1088/1748-9326/11/7/074005, 2016.

988 Shrestha, F., Steiner, J. F., Shrestha, R., Dhungel, Y., Joshi, S. P., Inglis, S., Ashraf, A., Wali, S., Walizada,
989 K. M., and Zhang, T.: HMAGLOFDB v1.0 – a comprehensive and version controlled database of glacier
990 lake outburst floods in high mountain Asia, *Earth Syst. Sci. Data Discuss.*, 2023, 1-28, 10.5194/essd-
991 2022-395, 2023.

992 Taylor, C., Robinson, T. R., Dunning, S., Rachel Carr, J., and Westoby, M.: Glacial lake outburst floods
993 threaten millions globally, *Nat Commun*, 14, 487, 10.1038/s41467-023-36033-x, 2023a.

994 Taylor, C. J., Robinson, T. R., Dunning, S., and Carr, J. R.: The rise of GLOF danger: trends, drivers and
995 hotspots between 2000 and 2020, *Authorea Preprints*, 2023b.

996 U.S. Army Corps of Engineers, I. f. W. R., Hydrologic Engineering Center, CEIWR-HEC: HEC-RAS river
997 analysis system. 2D modeling user's manual, Institute for Water Resources, Hydrologic Engineering
998 Center, Davis, USA, 289 pp.2021.

999 Uddin, K.: Land cover of HKH region, ICIMOD [dataset], 2021.

1000 Uddin, K., Matin, M. A., Khanal, N., Maharjan, S., Bajracharya, B., Tenneson, K., Poortinga, A., Quyen,
1001 N. H., Aryal, R. R., Saah, D., Lee Ellenburg, W., Potapov, P., Flores-Anderson, A., Chishtie, F., Aung, K. S.,
1002 Mayer, T., Pradhan, S., and Markert, A.: Regional Land Cover Monitoring System for Hindu Kush
1003 Himalaya, in: Earth Observation Science and Applications for Risk Reduction and Enhanced Resilience
1004 in Hindu Kush Himalaya Region: A Decade of Experience from SERVIR, edited by: Bajracharya, B.,
1005 Thapa, R. B., and Matin, M. A., Springer International Publishing, Cham, 103-125, 10.1007/978-3-030-
1006 73569-2_6, 2021.

1007 Wang, W., Zhang, T., Yao, T., and An, B.: Monitoring and early warning system of Cirenmaco glacial lake
1008 in the central Himalayas, *International Journal of Disaster Risk Reduction*, 73,
1009 10.1016/j.ijdr.2022.102914, 2022.

1010 Watanabe, T. and Rothacher, D.: The 1994 Lugge Tsho glacial lake outburst flood, Bhutan Himalaya,
1011 *Mountain Research and Development*, 16, 77-81, Doi 10.2307/3673897, 1996.

1012 World Bank: Bhutan - Institutional Strengthening and Modernization of Hydromet and Multi-hazard
1013 Early Warning Services in Bhutan : A Road Map for 2024-2034 (English) Institutional Strengthening and
1014 modernization of hydromet and multi-hazard early warning services in Bhutan: A road map for 2024
1015 to 2034, 2024.

1016 Zhang, G., Bolch, T., Yao, T., Rounce, D. R., Chen, W., Veh, G., King, O., Allen, S. K., Wang, M., and Wang,
1017 W.: Underestimated mass loss from lake-terminating glaciers in the greater Himalaya, *Nature*
1018 *Geoscience*, 10.1038/s41561-023-01150-1, 2023a.

1019 Zhang, G., Carrivick, J. L., Emmer, A., Shugar, D. H., Veh, G., Wang, X., Labeledz, C., Mergili, M., Mölg, N.,
1020 Huss, M., Allen, S., Sugiyama, S., and Lützw, N.: Characteristics and changes of glacial lakes and
1021 outburst floods, *Nature Reviews Earth & Environment*, 10.1038/s43017-024-00554-w, 2024.

1022 Zhang, G., Yao, T., Huss, M., Carrivick, J. L., Bolch, T., Li, X., Zheng, G., Peng, M., Wang, X., Steiner, J.,
1023 Rashid, I., Rinzin, S., Wangchuk, S., Sattar, A., Tiwari, R. K., Quincey, D., and Ali, F.: A monitoring network
1024 for mitigating Himalayan glacial lake outburst floods, *Bulletin of the American Meteorological Society*,
1025 10.1175/bams-d-24-0290.1, 2025.

1026 Zhang, T., Wang, W., An, B., and Wei, L.: Enhanced glacial lake activity threatens numerous
1027 communities and infrastructure in the Third Pole, *Nature Communications*, 14, 10.1038/s41467-023-
1028 44123-z, 2023b.

1029 Zheng, G., Mergili, M., Emmer, A., Allen, S., Bao, A., Guo, H., and Stoffel, M.: The 2020 glacial lake
1030 outburst flood at Jinwuco, Tibet: causes, impacts, and implications for hazard and risk assessment, *The*
1031 *Cryosphere Discuss.*, 2021, 1-28, 10.5194/tc-2020-379, 2021a.

1032 Zheng, G., Allen, S. K., Bao, A., Ballesteros-Cánovas, J. A., Huss, M., Zhang, G., Li, J., Yuan, Y., Jiang, L.,
1033 Yu, T., Chen, W., and Stoffel, M.: Increasing risk of glacial lake outburst floods from future Third Pole
1034 deglaciation, *Nature Climate Change*, 11, 411-417, 10.1038/s41558-021-01028-3, 2021b.

1035 Zhou, H., Wang, J. a., Wan, J., and Jia, H.: Resilience to natural hazards: a geographic perspective,
1036 *Natural Hazards*, 53, 21-41, 10.1007/s11069-009-9407-y, 2009.

1037